

# Paleoceanography and Paleoclimatology®









## RESEARCH ARTICLE

10.1029/2023PA004746

## Century-Long Records of Sedimentary Input on a Caribbean Reef From Coral Ba/Ca Ratios

### Key Points:

- Coral skeletal Ba/Ca measured by LA-ICP-MS is a proxy for river discharge and sediment flux to the reefs in this study
- Skeletal Ba/Ca has increased in forereef corals that mainly receive riverine flux from Honduras
- Results suggest that changing land-use around the Mesoamerican Barrier Reef System could be influencing long-term coral growth trends

Kathryn M. M. Shaw<sup>1,2,3</sup> , Christopher D. Standish<sup>1</sup> , Sara E. Fowell<sup>1,4</sup> , Joseph A. Stewart<sup>1,2</sup> , Karl D. Castillo<sup>5,6</sup> , Justin B. Ries<sup>7</sup> , and Gavin L. Foster<sup>1</sup> 

<sup>1</sup>School of Ocean and Earth Science, University of Southampton, National Oceanography Centre, Southampton, UK,

<sup>2</sup>School of Earth Science, University of Bristol, Bristol, UK, <sup>3</sup>Department of Earth Sciences, University of Cambridge, Cambridge, UK, <sup>4</sup>National Oceanography Centre, Southampton, UK, <sup>5</sup>Department of Earth, Marine, and Environmental Sciences, University of North Carolina at Chapel Hill, Chapel Hill, NC, USA, <sup>6</sup>Environment, Ecology, and Energy Program, University of North Carolina at Chapel Hill, Chapel Hill, NC, USA, <sup>7</sup>Department of Marine & Environmental Sciences, Marine Science Centre, Northeastern University, Nahant, MA, USA

### Supporting Information:

Supporting Information may be found in the online version of this article.

### Correspondence to:

K. M. M. Shaw,  
kms91@cam.ac.uk

### Citation:

Shaw, K. M. M., Standish, C. D., Fowell, S. E., Stewart, J. A., Castillo, K. D., Ries, J. B., & Foster, G. L. (2024). Century-long records of sedimentary input on a Caribbean reef from coral Ba/Ca ratios. *Paleoceanography and Paleoclimatology*, 39, e2023PA004746. <https://doi.org/10.1029/2023PA004746>

Received 23 AUG 2023

Accepted 4 MAR 2024

### Author Contributions:

**Conceptualization:** Kathryn M. M. Shaw, Christopher D. Standish, Sara E. Fowell, Gavin L. Foster

**Data curation:** Kathryn M. M. Shaw, Christopher D. Standish, Sara E. Fowell

**Formal analysis:** Kathryn M. M. Shaw, Christopher D. Standish, Sara E. Fowell, Joseph A. Stewart

**Funding acquisition:** Gavin L. Foster

**Investigation:** Kathryn M. M. Shaw, Christopher D. Standish, Sara E. Fowell, Joseph A. Stewart, Gavin L. Foster

**Methodology:** Kathryn M. M. Shaw, Christopher D. Standish, Sara E. Fowell, Joseph A. Stewart, Karl D. Castillo, Justin B. Ries, Gavin L. Foster

**Project administration:** Gavin L. Foster

**Abstract** Coral reef ecosystems are delicately balanced and are thus prone to disruption by stressors such as storms, disease, climate variability and natural disasters. Most tropical coral populations worldwide are now in rapid decline owing to additional anthropogenic pressures, such as global warming, ocean acidification and a variety of local stressors. One such problem is the addition of excess sediment and nutrients flux to reefs from increased soil erosion from land use changes. Here we present century-long Ba/Ca records from two *Siderastrea siderea* colonies as a proxy for local riverine discharge and sediment flux to the southern Mesoamerican Barrier Reef System (MBRS). The coral colonies have linear extension trends, which can be seen as a first-order indicator for coral health and response. The coral colony that exhibits a decline in linear extension rate from the forereef of the MBRS, mainly receives riverine input from Honduras, whilst the coral from the backreef, which does not exhibit a decline in extension rate, primarily receives riverine input from more sparsely populated regions of Belize. Coral Ba/Ca increased (>70%) through time in the forereef colony, while the backreef colony showed little long-term increase in Ba/Ca over the last century. Our results suggest that increasing sediment supply may have played a role in the decline of forereef skeletal extension in the southernmost MBRS region, likely stemming from increasing land-use changes in Honduras.

## 1. Introduction

Coral reefs are increasingly at risk from multiple anthropogenic pressures, such as rising sea surface temperatures (SSTs), ocean acidification, over-fishing, increasing sedimentation and nutrients, and increasing pollutants (Hoegh-Guldberg et al., 2007). Coupled with natural stressors, such as climate variability, disease, and storms, these anthropogenic pressures have led to an extensive decline of coral ecosystems worldwide (Knowlton & Jackson, 2008). Over 25% of reefs worldwide are currently threatened by excess land-derived sediment and nutrient input (eutrophication) resulting from land-use and/or hydrological changes (Burke & Sugg, 2006; Fabricius, 2005). Suspended and settling sediment both reduce light availability for photosynthesis and smother the coral organism (Rogers, 1990). Eutrophication resulting from nutrients accompanying the suspended sediments can trigger fleshy macroalgae blooms, which outcompete stony corals and can cause localized hypoxia (Ogden & Ogden, 1998). As human populations in coastal regions continue to increase, land clearance, coastal development, and agriculture all promote the delivery of sediments, as well as fertilisers and pesticides, to rivers and coastal waters. These regional stressors are therefore a considerable threat to the world's coral reefs, but unlike global phenomena such as ocean warming and acidification, regional stressors are more easily managed and mitigated. However, in the absence of detailed observational records, the history of sediment delivery to reefs and its role in regional coral decline remain unclear.

Here we examine differences in riverine Ba-supply, a tracer of terrigenous flux (McCulloch et al., 2003), between the forereef and backreef corals of the southern Mesoamerican Barrier Reef System (MBRS). Coral “FR-12” is part of the ocean-facing forereef and is thought to receive terrestrial flux mainly from the larger and more populated Honduran and Guatemalan watersheds south of the MBRS, whereas coral “BR-06” is in the more sheltered backreef zone of the reef that faces the Belizean coastline, and so receives its terrestrial flux predominantly from the smaller and less-populated watersheds of Belize (Burke & Sugg, 2006; Cherubin et al., 2008; Paris & Cherubin, 2008; Soto et al., 2009). Modelling of the regional watersheds (Honduras, Guatemala, Belize

© 2024. The Authors.

This is an open access article under the terms of the [Creative Commons Attribution License](https://creativecommons.org/licenses/by/4.0/), which permits use, distribution and reproduction in any medium, provided the original work is properly cited.

**Resources:** Karl D. Castillo, Justin B. Ries, Gavin L. Foster  
**Supervision:** Christopher D. Standish, Gavin L. Foster  
**Validation:** Kathryn M. M. Shaw  
**Writing – original draft:** Kathryn M. M. Shaw  
**Writing – review & editing:** Kathryn M. M. Shaw, Christopher D. Standish, Sara E. Fowell, Joseph A. Stewart, Karl D. Castillo, Justin B. Ries, Gavin L. Foster

and Mexico) along the MBRS shows that 80% of sediment, 55% of nitrate and 60% of phosphate delivered to the reef comes from Honduras, with the Ulúa River contributing the greatest flux of all modelled watersheds (Burke & Sugg, 2006). Rapid increase in human population alongside increases in agricultural activity, particularly in Honduras (Figure 2), has led to deforestation and an increase in the use of fertilisers, herbicides and pesticides (United-Nations, 2020). These factors have likely increased the flux of sediments, and nutrients and other chemical stressors to the forereef of the MBRS; a factor that could be contributing to a documented decline in skeletal linear extension in the forereef corals relative to backreef corals (Castillo et al., 2011). Despite their proximity, Belize watersheds contribute negligible sediment, less than 12% of the nutrients found in the local seawater and have experienced less population growth than the adjacent Honduran watersheds (Figure 2), raising the possibility that backreef corals are at lower risk of degradation from these factors than forereef corals (Burke & Sugg, 2006). To test this, we present 100-year records of the Ba/Ca ratio of two coral cores to reconstruct the riverine flux to each side of the reef crest on the southern MBRS and use this archive to assess the potential impact of riverine flux on reef health in the region since the early 1900s.

### 1.1. Study Area

Our study area is in the southern portion of the Mesoamerican Barrier Reef System (MBRS) within the Sapodilla Cayes Marine Reserve, located in the Caribbean Sea off the coasts of Belize, Guatemala, Honduras, and Mexico. Coral decline in the Caribbean is particularly severe with 50% or more coral cover lost since observations started in the 1970s (Cramer et al., 2020; Jackson et al., 2014). These patterns of decline are not uniform across the Caribbean, with coral mortality more pronounced in areas where local stressors are prominent (Jackson et al., 2014). Areas particularly impacted by pollution, overfishing and tourism are characterized by the most rapid collapse of reef ecosystems (Baker et al., 2010; Carilli, Prouty, et al., 2009; Guzman & Jimenez, 1992; Rogers, 1983; Sutherland et al., 2010). Furthermore, some well-managed reefs have regrown after major stress events, highlighting the importance of monitoring these local stressors to limit reef decline in the Caribbean (Jackson et al., 2014).

The coral cores for this study were extracted from two living large mounding *Siderastrea siderea* coral colonies ~21 km apart in the Sapodilla Cayes Marine Reserve in the southern MBRS (Figure 1; FR-12, 16.13715°N, 88.26015°W; BR-06, 16.14045°N, 88.26015°W). As a marine reserve since 1996, fishing has been restricted in this region and dredging is minimal, leaving land-derived pollution (i.e., eutrophication, sedimentation, changes in salinity) from riverine input and global stressors (e.g., ocean acidification, rising SSTs) as the greatest threats facing corals in the area. Seasonal cycles in SST are minor at this site (Figure 5, 26°C to 30°C January to July). The Central American wet season (May to November) provides up to 5,000 mm/year of precipitation annually (Horel, 1982; Thattai et al., 2003).

### 1.2. Previous Work on Coral Cores From the MBRS

One metric for assessing coral health is skeletal linear extension rate, estimated from the widths of coupled high- and low-density pairs of annual growth. This is seen as a health indicator given the intimate relationship between total skeletal extension and calcification rates within *S. siderea* (Carricart-Ganivet et al., 2013; De'ath et al., 2009). Using this approach Castillo et al. (2011) found that, over the last 100 years, there has been a decline in linear extension of seven *S. siderea* corals from the forereef (including colony FR-12; this study) of the MBRS, decreasing by an average of around 0.2 mm/year, while extension in the backreef (including colony BR-06; this study) increased by 0.1 mm/yr. Contrasting trends in extension rates between corals of the same species in relatively close proximity (Figure 1) but subject to different environmental stressors, therefore, allow for an in-depth case-study investigating the environmental parameters responsible for the observed changes in coral reef growth.

Previous geochemical measurements of the coral cores suggest that many environmental conditions experienced by these corals were similar over the last 80 years. Temperature-sensitive coral Li/Mg and Sr/Ca data from the forereef and backreef reveal the regions experienced similar thermal histories over the last century (only +1°C summer warming since 1922; Fowell et al. (2016)). If long-term temperature increase were the primary stressor leading to extension rate decline in the forereef, we would expect to see more intense warming with time in this coral colony. Furthermore, the backreef generally experiences slightly warmer and more variable SST temperatures than the forereef due to its more isolated reef position from the open ocean which would suggest the backreef coral would be more prone to sub annual heating or bleaching events over the last century (Castillo

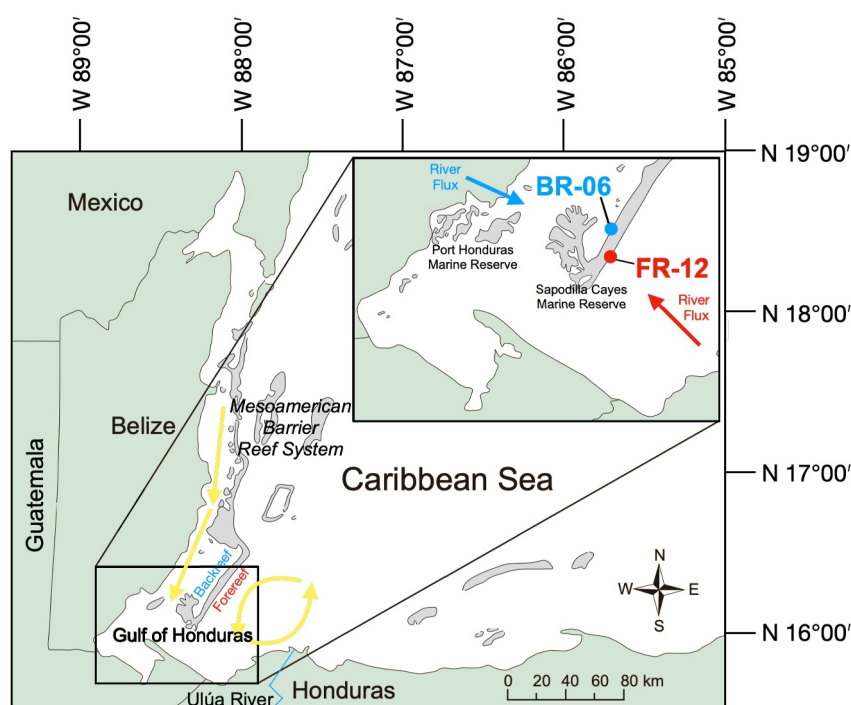


**Figure 1.** The two cored *Siderastrea siderea* coral colonies, BR-06 and FR-12, are from the backreef and forereef, respectively (Sapodilla Cayes Marine Reserve). The MBRS lies off the coasts of Belize, Guatemala, Honduras, and Mexico. Ocean current patterns discussed in text are highlighted in yellow (Cherubin et al., 2008). The Ulúa River (Honduras), indicated by the blue line, is also highlighted as the greatest contributor of sediment and nutrients to the reef system.

et al., 2011). Additionally, in contrast to what would be expected from the relationship between ocean acidification and coral calcification, skeletal boron isotope pH-proxy data suggest that the backreef coral that exhibited more stable rates of extension through time experienced the most ocean acidification over the last ~100 years, while the forereef coral that exhibited a decline in extension rate through time experience little long-term change in seawater pH (Fowell et al., 2018). Together, these studies suggest that differential temperature and pH stress are not responsible for the disparity in coral growth rate trends between the forereef (declining growth) and backreef (stable growth) colonies.

### 1.3. Ba/Ca Proxy

The Ba/Ca ratio in coral skeletons is an established proxy for riverine flux and sediment delivery to coral reefs (McCulloch et al., 2003). As coral grows, divalent cations such as  $Ba^{2+}$  are incorporated into the skeletal aragonite from ambient seawater via lattice substitution for  $Ca^{2+}$ . Trace element variation within coral skeletons can therefore reflect changes in contemporaneous seawater chemistry, and, if incorporation is dependent on environmental variables (e.g., temperature or pH) past conditions can also be reconstructed (Gaetani & Cohen, 2006; Gaetani et al., 2011; LaVigne et al., 2011, 2016; Lea et al., 1989; Spooner et al., 2018).

Barium concentrations in seawater ( $[Ba]_{sw}$ ) have a nutrient-like profile and are generally low in open ocean surface waters ( $[Ba]_{sw} \sim 40$  nmol/kg; Chan et al. (1977)). High open ocean  $[Ba]_{sw}$  is generally restricted to upwelling zones where Ba returns to the surface following its remineralization at depth (Lea et al., 1989). In coastal regions, rivers are a principal supply vector for Ba alongside coastal upwelling (Ourbak et al., 2006). As salinity increases when riverine water mixes with coastal seawater,  $[Ba]_{sw}$  becomes elevated as Ba desorbs from particulate matter in the estuarine zone (Brenner et al., 2017; Hanor & Chan, 1977; Sinclair & McCulloch, 2004). While salinity gradients cause  $[Ba]_{sw}$  to increase in estuaries, fluctuations in sea surface salinity (SSS) within the vicinity of calcifying stony corals do not seem to directly affect Ba incorporation in stony coral skeletons (Pretet et al., 2014). Thus, variations in Ba/Ca are typically attributed to the increased supply of  $Ba^{2+}$  (relative to  $Ca^{2+}$ ) to coral colonies rather than changing salinity. If skeletal coral Ba/Ca varies directly with Ba/Ca in seawater with no supplementary controlling factors (e.g., temperature or Rayleigh fractionation in the calcifying fluid), Ba/Ca in

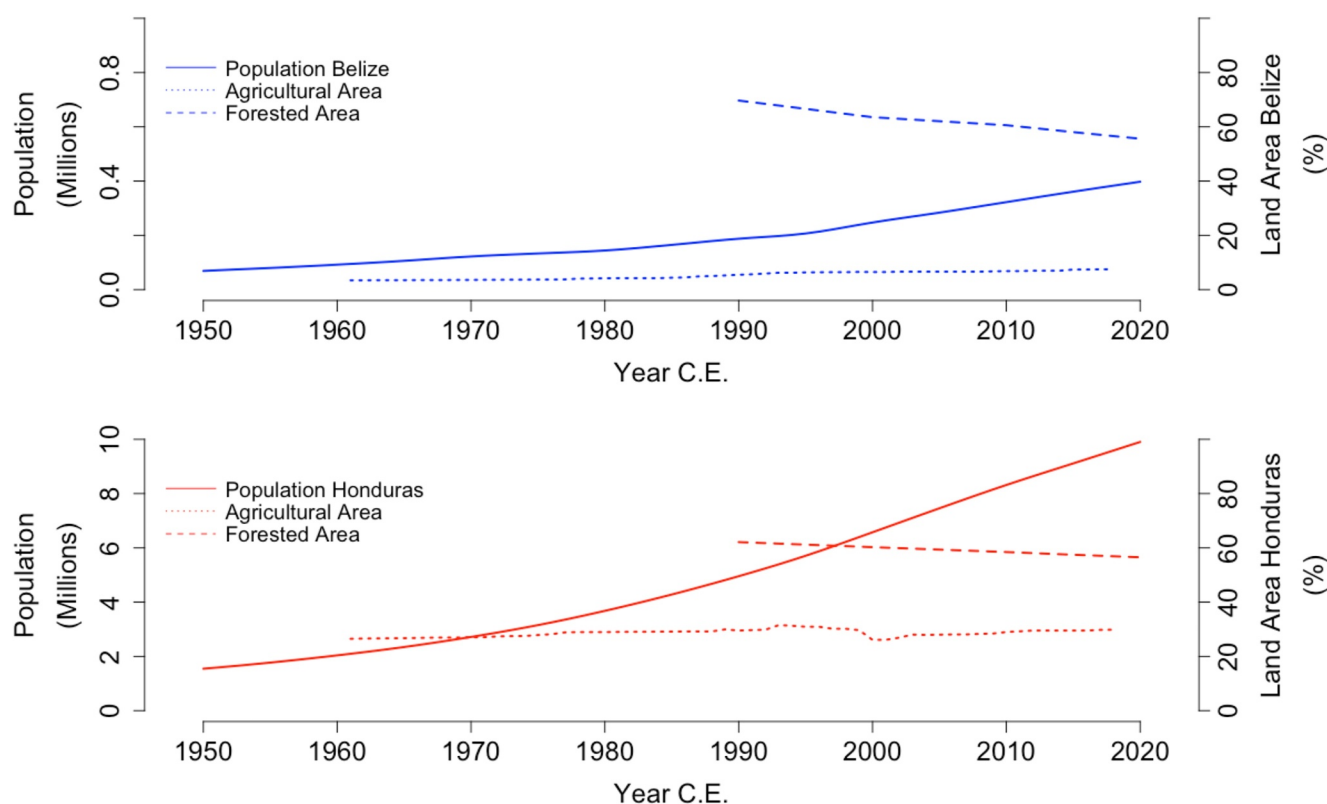


**Figure 2.** Contrasting changes in human population (solid), forest land cover (dashed), and agricultural land area (dotted) in Belize (blue, top panel) and Honduras (red, bottom panel) over the last 70 years (United-Nations, 2020).

coastal coral skeleton should reflect changes in Ba supply in riverine plume load and sediment delivery to coastal waters (McCulloch et al., 2003).

Indeed, several studies have shown that coral Ba/Ca reflects periodic climatic cycles such as the El Niño Southern Oscillation (ENSO) (Maina et al., 2012), and short-scale irregular weather events (e.g., storms and regional precipitation; Prouty et al. (2010)). In tropical regions, precipitation and the hydrological cycle are controlled by the seasonal movement of the inter-tropical convergence zone (ITCZ). The northward movement of the ITCZ in boreal summer generates the Central American wet season (May to November), providing up to 5,000 mm/year of precipitation (Horel, 1982; Thattai et al., 2003). This seasonality manifests as yearly oscillations in Ba/Ca records in Caribbean coral skeletons (Brenner et al., 2017; Horta-Puga & Carriquiry, 2012). Conversely, shallow coral colonies calcifying further away from direct river sources can reflect  $[Ba]_{sw}$  related to upwelling and the removal of Ba from the water column via biological activity (Carter et al., 2020).

There are cases in which spatially and temporally coincident corals can display disparate Ba/Ca records, with little or no link to local riverine variability (Lewis et al., 2018; Sinclair, 2005). As a result,  $Ba/Ca_{sw}$  variability has been ascribed to other localized phenomena such as Ba sources from upwelling (Lea et al., 1989), barite formation accompanying phytoplankton blooms (Saha et al., 2018; Sinclair, 2005), and Ba release from sediment resuspension (Prouty et al., 2010). However, anthropogenic forcing and pollution have also been linked to Ba/Ca variability such as groundwater discharge (Prouty et al., 2010; Rosenheim et al., 2005), dam collapse (Cardoso et al., 2022), land use change (Carilli, Prouty, et al., 2009), and oil pollution (Carriquiry & Horta-Puga, 2010; Weerabaddana et al., 2021). These disparities in Ba supply, as well as biologically induced fractionation in trace element incorporation within coral skeletons (Dietzel et al., 2004; Gaetani & Cohen, 2006; Lea et al., 1989), reinforce the need to cautiously approach Ba/Ca as a proxy for river sediment supply.

## 2. Materials and Methods

### 2.1. Sample Collection and Preparation

The two coral cores used in this study were extracted within the Sapodilla Cayes Marine Reserve in February 2009; see Castillo et al. (2011) for full details. Briefly, cores up to 100 cm in length, and 5 cm in diameter were extracted by SCUBA using a 2-horsepower hand-held pneumatic core drill affixed with a hollow extension rod (5 cm in diameter, 90 cm in length) and a wet diamond core bit (5 cm in diameter, 30 cm in length). The cores were collected from the center of each coral colony parallel to the coral's vertical growth axis and subsequently cleaned with 95% ethanol. Corals were chosen from the ocean-facing forereef and from the Belizean coast-facing backreef from living colonies that appeared healthy and were without any obvious abnormalities, scarring, bleaching, or disease at a water depth of between 3 and 5 m (Figure 1). The hardy, reef-building, zooxanthellate coral species *S. siderea* was selected for its long lifespan and slow growth allowing for long paleoceanographic records. This species inhabits shallow to moderate depth environments and is capable of surviving extreme stress (Guzman & Tudhope, 1998). This resilience is further confirmed by a lack of obvious hiatuses in the annual banding of the cores studied here.

### 2.2. Age Model for Ba/Ca and Luminescence

An initial age model at annual resolution was constructed using X-ray imagery assuming a bright/dark couplet representing a single year with low density skeleton deposited over the dry season (December to May). *S. siderea* grow radially and a core taken along the growth axis should reflect the growth history of the coral. The top of the core where the polyp resided was taken as the date of collection (February 2009). By taking the initial x-ray age models we then generate a new, seasonally resolved age model for both cores using cyclicity in measured skeletal Ba/Ca, tuning the peak Ba/Ca to July, and troughs in Ba/Ca to February, as shown to be valid by the x-ray age model. By tuning the Ba/Ca to its own seasonality we negate any effect that imperfect slabbing may have on the Ba/Ca proxy in terms of temporal resolution. A high order polynomial was fitted between the distance and season data (two tie points per year) to give a continuous age model accounting for the changing growth rates between each year. Any hiatuses in the coral core were due to physical breakage of the core after collection and were assumed to be small enough that less than a full cycle was lost (<5 mm, ~average year). Any part-cycle lost was then estimated by linear interpolation of the age model.

### 2.3. Trace Element Data Collection

#### 2.3.1. Laser Ablation ICP-MS

Each core was cut to fit a 100 mm by 100 mm laser ablation cell; BR-06 was cut into 8 sections and FR-12 was cut into 6 sections. Sections were polished and washed in an ultrasonic bath before being mounted level on 75 mm by 45 mm glass slides. Core sections were cut at shallow angles across the growth axis. This allowed for overlap of the laser tracks between sections along the growth (temporal) axis to ensure a smooth assembly of the element profiles between sections by matching the overlapping cycles, avoiding gaps related to the sectioning (Figure S1 in Supporting Information S1).

The cores were analyzed for trace elemental composition ( $^{24}\text{Mg}$ ,  $^{43}\text{Ca}$ ,  $^{137}\text{Ba}$ ) using laser ablation inductively coupled plasma mass spectrometry (LA-ICP-MS). This approach was employed for its time efficiency for generating high spatial-resolution (sub-millimeter) results in situ from coral sections (Sinclair et al., 1998; Sylvestre, 2008). Coral cores were mounted on the laser stage alongside the National Institute of Standards and Technology (NIST) glass reference materials SRM 612 and SRM 610.

Laser ablation analysis was performed on a Thermo Scientific X-Series II Quadrupole ICP mass spectrometer coupled to an Elemental Scientific NWR193 excimer laser ablation system with a TwoVol2 ablation chamber. Operating conditions are detailed in Table S8 in Supporting Information S1. Each coral laser transect was split into three measurement divisions allowing frequent bracketing with reference materials, for a total of four brackets per core segment. A continuous line transect reduces the likelihood of downhole (z-axis) elemental fractionation whilst maximizing the spatial resolution along the growth axis. Transects followed theca walls, avoiding the columella that exhibit variations in some elemental ratios (e.g., Chalk et al. (2021); DeLong et al. (2016)). Surface topography with a high aspect ratio was also avoided to reduce any potential laser-induced elemental fractionation effects between volatile and refractory elements (Sinclair et al., 1998). Blank, instrumental drift and mass bias corrections were applied offline. The average background intensities for  $^{137}\text{Ba}$ ,  $^{24}\text{Mg}$ , and  $^{43}\text{Ca}$  were <<1% of the sample



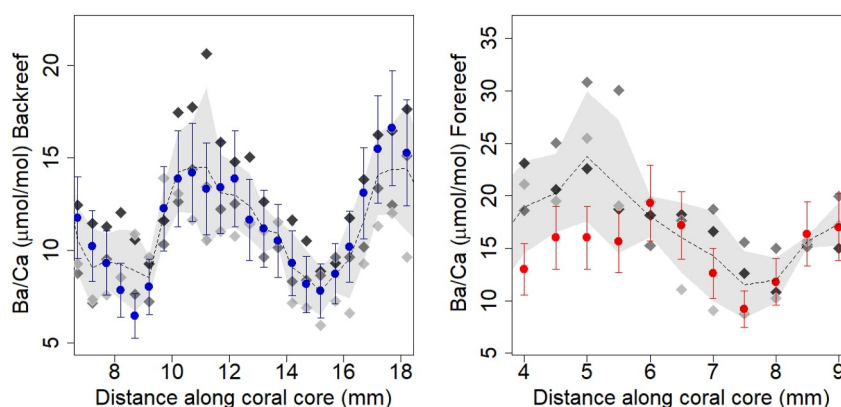


**Figure 3.** Agreement between laser-ablation and milling techniques. Ba/Ca data (light and dark gray diamonds) obtained from replicate laser lines compared to that obtained from solution ICP-MS data (blue circles) on the upper section of each coral core, showing the replication of seasonal cycles (core top = 0 mm). The uppermost tissue layer is excluded due to elevated Ba/Ca from organic tissue contamination. Error bars represent %RSD of the solution data. Laser data are averaged into 0.5 mm bins comparable to the 0.5 mm vertical distance of core sampled for each solution measurement. Dashed line and gray shaded band represent the mean and 1 SD, respectively, of the four data points (laser and solution) for each 0.5 mm bin. Both BR-06 (left) and FR-12 (right) exhibit temporally consistent peaks and troughs within each core, suggesting the Ba/Ca seasonality is apparent and replicable throughout the cores.

signal. Elemental ratios were calculated by ratioing to  $^{43}\text{Ca}$  (Sinclair et al., 1998) and normalizing to certified values for NIST SRM 612. The reproducibility of the Ba/Ca in NIST SRM 612 was 6.74% RSD (2SD) across all 7 analytical sessions. The external reproducibility of the coral data is given by repeat measurement of the NIST SRM 610 in each session (Data Set S1). For Ba/Ca, this ranges from 1.8% to 8.3% RSD (2SD).

Using a similar approach to Marks et al. (2017) and Sinclair et al. (2011) to reduce analytical noise, a 40-point (35  $\mu\text{m}$  window) running mean was applied to coral Ba/Ca as it yielded the greatest reproducibility between repeat line-transects (Welch's unequal variance paired  $t$ -test,  $p > 0.05$ ). For all laser ablation data, values outside of three times the interquartile range were identified as outliers and removed (<0.01% of data).

### 2.3.2. Solution ICP-MS and Accuracy of Laser Ablation Data

Selected samples from the uppermost growth bands of the coral were taken and measured for Ba/Ca by solution ICP-MS to validate the accuracy of higher spatial resolution laser ablation data. We chose the uppermost section of core to contrast against the high Ba/Ca observed in the organic layer between solution and laser measurements (see below). A New Wave Research micromill with a 500  $\mu\text{m}$  diameter diamond drill bit was used to drill trenches to a depth of 1 mm in the theca wall using a protocol similar to that of DeLong et al. (2011). Theca wall widths were identified under the microscope to minimize the possibility of sampling columellae. Powdered samples were typically 1 mg in mass. Residual organic matter was removed from powders using warm 1%  $\text{H}_2\text{O}_2$  (80°C; buffered in  $\text{NH}_4\text{OH}$ ) and a weak acid leach (0.0005 M  $\text{HNO}_3$ ) (Boyle, 1981) before dissolution in distilled 0.5 M  $\text{HNO}_3$ . Using a method similar to Marchitto (2006), an aliquot of the dissolved sample was analyzed using a Thermo Scientific Element XR ICP mass spectrometer using well-characterized, matrix-matched (80  $\mu\text{g/g}$  [Ca]), synthetic standard solutions to yield Ba/Ca. The international coral reference material JCp-1 (made from homogenised *Porites* by the Japanese Geological Survey; Okai et al. (2002)) was cleaned and analyzed simultaneously with the coral samples to provide an assessment of external reproducibility. The mean measured Ba/Ca of JCp ( $n = 16$ ) was  $6.41 \pm 1.26$   $\mu\text{mol/mol}$  ( $\pm 9.8\%$ ;  $\pm 2\sigma$ ), which falls in the range of values reported from an interlaboratory study, where the mean Ba/Ca was  $7.47 \pm 1.32$   $\mu\text{mol/mol}$  (Hathorne et al., 2013).

Accuracy of laser ablation is demonstrated by two approaches. First, Ba/Ca and Mg/Ca measurements of NIST SRM 610 normalized to NIST SRM 612 are within uncertainty (2SD) of literature values compiled from Evans and Muller (2018) (Data Set S1). Second, laser Ba/Ca measurements were performed adjacent to sampling for solution ICP-MS analyses on both FR-12 and BR-06. Three repeat laser transects from both core tops were aligned and averaged into 0.5 mm bins for more direct comparison to solution ICP-MS data from 0.5 mm drilled trenches. Figure 3 shows the agreement in laser and solution Ba/Ca data. Similar cycles in Ba/Ca are evident in

both the solution and laser data sets, but there is some discrepancy in the magnitude of the cycles, potentially relating to the small scale variation in Ba/Ca recently observed between thecal walls and columella, with the latter more readily sampled by the solution ICP-MS method (Chalk et al., 2021). The mean RMSE for Ba/Ca between each laser line and the solution data was 3.8  $\mu\text{mol/mol}$ , ranging between 1.6  $\mu\text{mol/mol}$  and 2.7  $\mu\text{mol/mol}$  for the backreef and between 4.3  $\mu\text{mol/mol}$  and 7.4  $\mu\text{mol/mol}$  for the forereef. This signifies that the NIST SRM 612 corrected LA-ICP-MS data record the same variations as the solution-based data in the uppermost section of the corals, even across different corallites. Internal reproducibility (2SD) of the laser repeated core top transects yielded at worst a range of 5.2  $\mu\text{mol/mol}$  ( $\sim 35\%$ ,  $n = 3$ ) and 6.5  $\mu\text{mol/mol}$  ( $\sim 29\%$ ,  $n = 3$ ) for the backreef and forereef colonies, respectively.

#### 2.4. Luminescence Profiles

Under UV light, sectioned cores of both colonies display paired bands of luminescence (see Figure S1 in Supporting Information S1). Each couplet consists of a fluorescent band (wet season) and a dull band (dry season), which together represent a year of growth (Kaushal et al., 2020; Lough, 2011b). This banding is assumed to be caused by humic-like acids sourced from riverine flux incorporated into the growing coral skeleton. Given the proximity of both colonies to riverine input, it is likely that there will be temporal similarities between the data for the fluorescent banding and the Ba/Ca data, if Ba/Ca represents sediment input to the reef (Grove et al., 2010; McCulloch et al., 2003). Coral core sections were lightly polished and cleaned using MQ-water in an ultrasonic bath to remove any residual organic particles prior to fluorescence measurements. Once clean the cores were placed individually under UV light before a static camera photograph was taken at a set distance. Photos were converted into 8-bit greyscale images with pixels assigned a value between 0 (black) and 255 (white) using the software Fiji-ImageJ. The greyscale formula is independent of color and is solely a function of individual pixel brightness (i.e., fluorescence of the coral). A continuous profile was constructed by sampling greyscale values following the path of the laser transect. Monthly means were then calculated based on the age model described above. To account for error when taking photographs individually rather than as a complete core, and to help negate the luminescent effect from the background age density artifact (Lough, 2011b), a new profile was then constructed by calculating the consecutive differences in the mean from 1 month to the next. Thus, increasing luminescence month to month is represented by positive values, and decreasing luminescence is represented by negative values. Although this approach removes any long-term trend in luminescence (if present), it retains relative difference caused by humic acid input on a monthly scale for comparison with Ba/Ca and effectively normalizes the greyscale values between images and cores.

#### 2.5. Statistical Analysis and Data Processing

Statistical analysis was carried out in R (R-Core-Team, 2019) or using PAST 4.03 (Hammer et al., 2001). Initially, Ba/Ca and luminescence results were binned into two-monthly averages as analysis at a higher temporal resolution was not required. This also reduced uncertainty associated with using a high temporal resolution from the polynomial fit of the age model versus the varying growth of the coral. Seasonality was removed to observe longer trends (frequencies up to and including annual) using a FIR low pass filter in PAST 4.03. From these decomposed data (without annual/seasonal cycles), recurring higher frequency cycles were identified using periodogram analysis. Another FIR filter removing all frequencies up to 25 years was also used, in combination with a loess trend line, to highlight long-term trends resulting from changes in Ba/Ca. Cross-correlations were done using the “CCF” functions from the package *tseries* (Trapletti & Hornik, 2020). Cox-Stuart trend tests and Buishand range tests were calculated using the *Trend* package (Pohlert, 2020).

### 3. Results

#### 3.1. Ba/Ca

Coral core FR-12 produced a continuous record from May 1922 to January 2009, assuming no gaps between core sections, with a maximum Ba/Ca of 20.2  $\mu\text{mol/mol}$ , a minimum of 3.8  $\mu\text{mol/mol}$  and a mean of 9.3  $\mu\text{mol/mol}$  ( $\pm 6.4$   $\mu\text{mol/mol}$ , 2SD). BR-06 produced a record from May 1908 to January 2009 with a maximum Ba/Ca of 24.1  $\mu\text{mol/mol}$ , a minimum of 2.6  $\mu\text{mol/mol}$  and a mean of 8.2  $\mu\text{mol/mol}$  ( $\pm 6.2$   $\mu\text{mol/mol}$ , 2SD) and three distinct gaps in the record where the coral core had been broken after collection, corresponding to dates in 1962, 1974, and 1995 (Figure 4). Ba/Ca spikes up to 1000  $\mu\text{mol/mol}$  found at the top  $\sim 1$  cm of the cores coinciding with

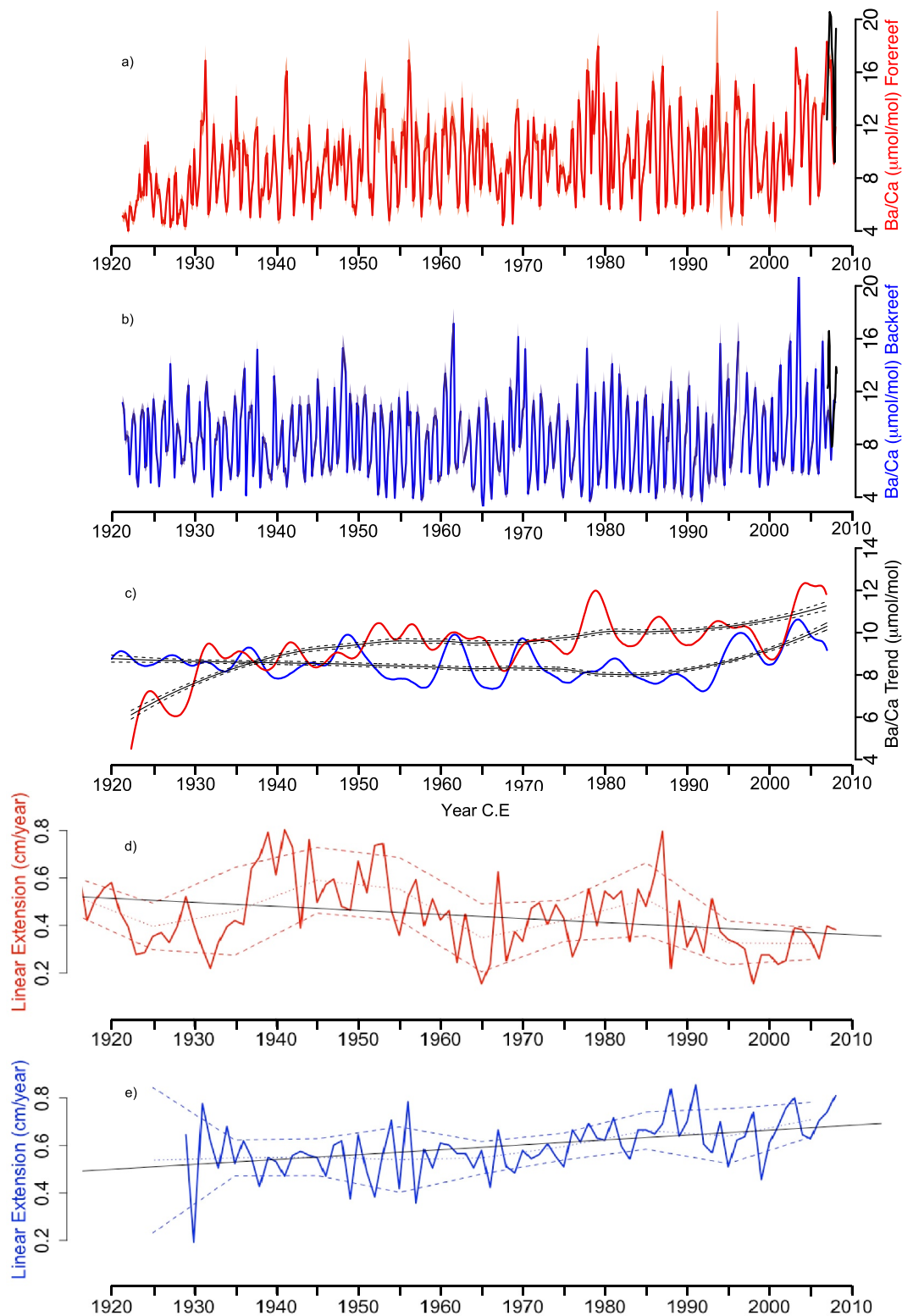


**Figure 4.** Monthly resolved Ba/Ca for backreef (BR-06; blue) and forereef (FR-12; red) corals with solution ICP-MS data (black) (a, b). Error (1SD) is shown as lighter bands around the solid lines. Decomposed loess trendlines (black) with cycles up to 25 years removed using a low pass FIR-filter for both BR-06 and FR-12 (c). Extension data for the two cores (d: FR-12 red, e: BR-06 blue) from Castillo et al. (2011). Dotted and dashed lines represent decadal mean and associated standard deviations (2SD) respectively. Solid black lines are linear regressions through decadal means.



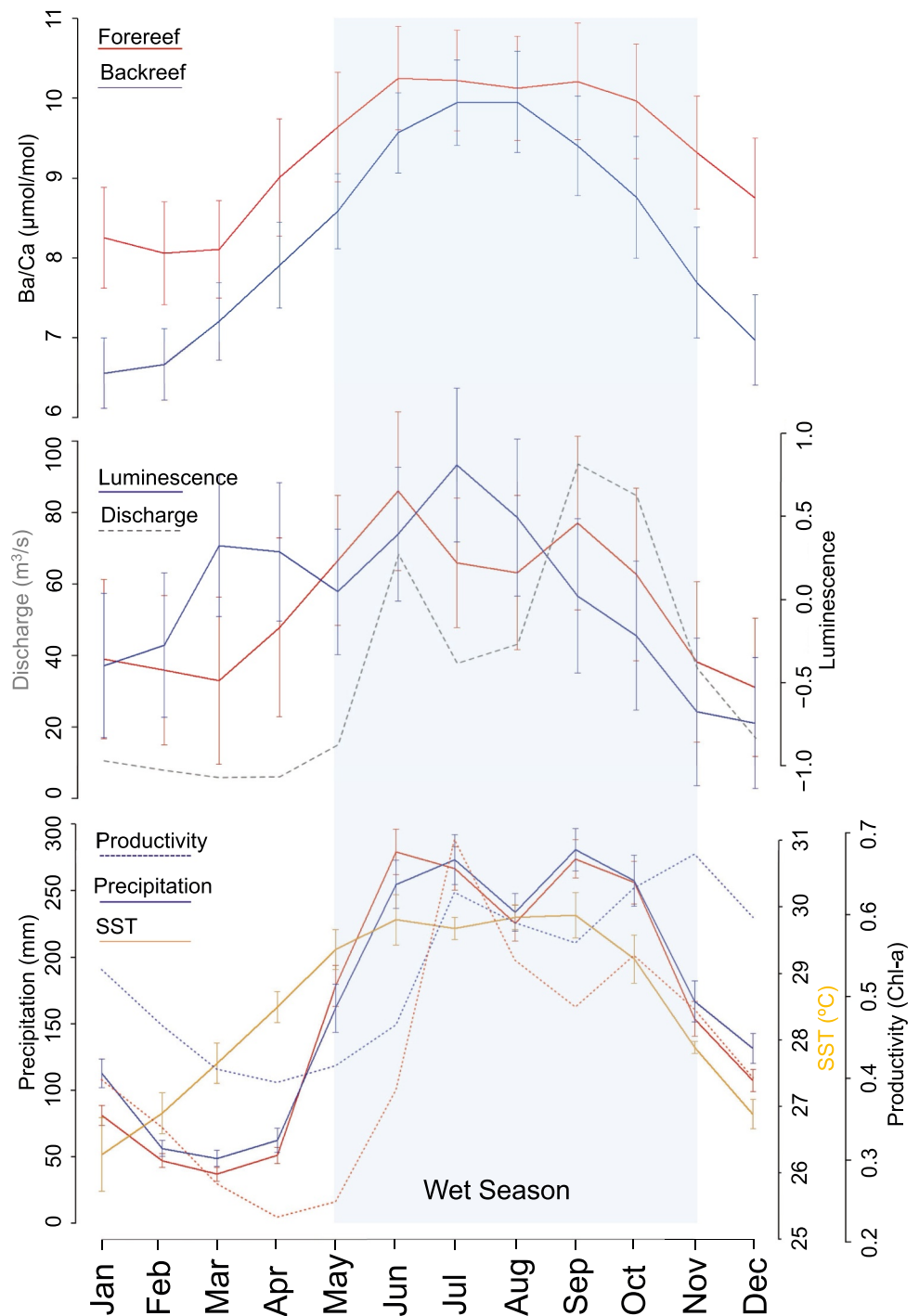


**Figure 5.** Monthly average Ba/Ca, luminescence, and precipitation from 1922 to 2006. Monthly average temperature from in situ loggers from 2002 to 2006 from Castillo and Lima (2010); see Castillo et al. (2012) and Fowell et al. (2016) for more details. Rainfall data are a gridded product from Honduras (red) and Belize (blue) (Harris et al., 2020). Productivity data are chlorophyll-a concentrations for the area around the forereef, 16.000–16.300°N, 88.100–87.800°W; and backreef, 16.200–16.500°N, 88.300–88.000°W from *Ocean Color CCI*; Sathyendranath et al. (2019). River discharge data are from *The Global Runoff Data Center*, 56068 Koblenz, Germany. Error bars represent 2 SE. Shaded area represents the wet season in the MBRS.

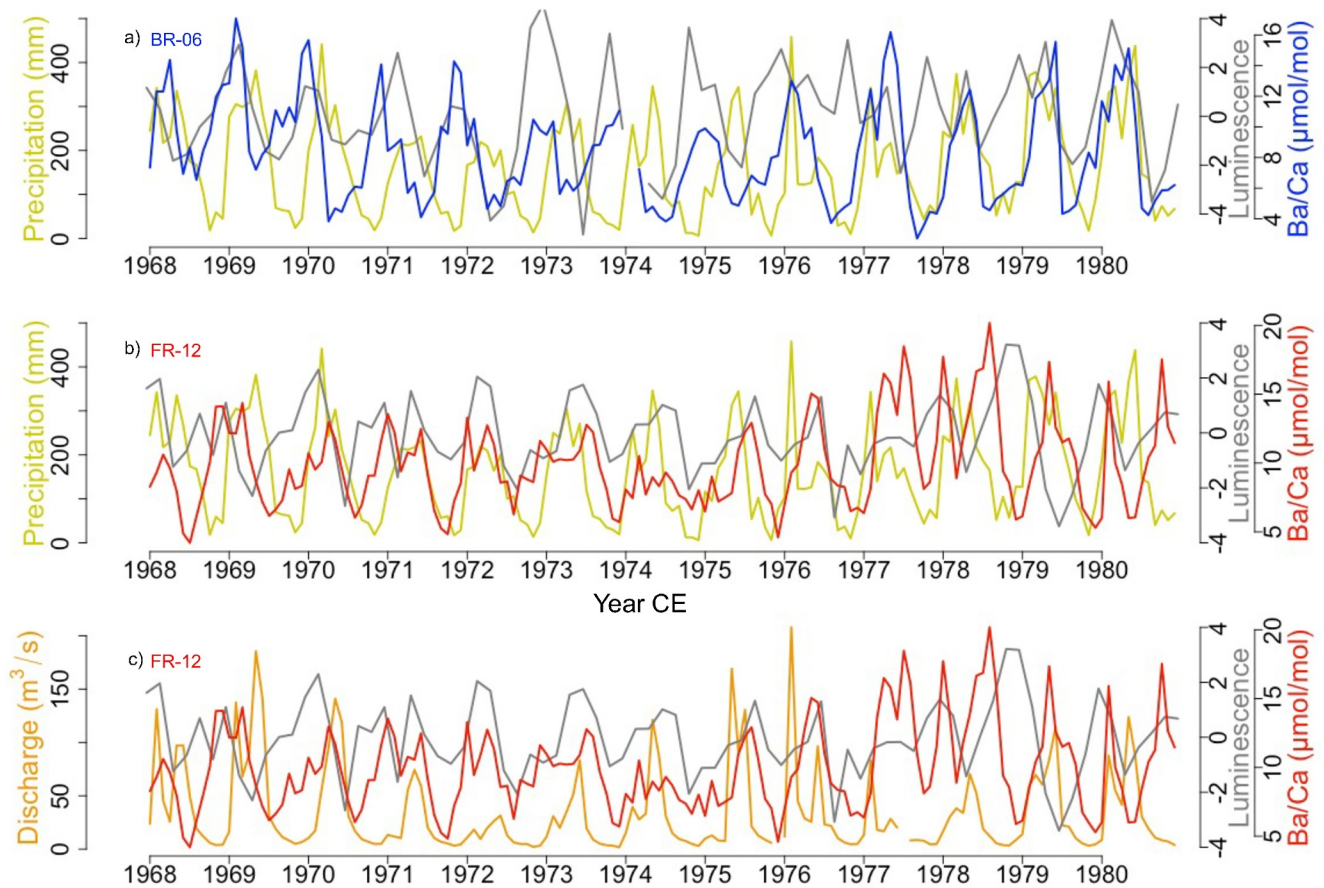


**Figure 6.** Comparing luminescence, rainfall, Ba/Ca, and discharge for a period which all data are available. Monthly difference in luminescence through the coral cores is defined by the gray lines alongside the Ba/Ca of the same core and gridded precipitation data for the region (Harris et al., 2020) (red FR-12, blue BR-06) (a, b). Discharge from a station on the Rio Humuya, flowing eventually into the Ulúa in Honduras (GRDC, 2022), and the Ba/Ca and luminescence within this study (FR-12 in red) (c). There is generally good correlation between the data sets but the Ba/Ca peaks drift in the time-series shown suggesting our age model has over/underestimated the growth between years for the Ba/Ca. We do not have river discharge data to compare directly to the backreef.

the discolored brown tissue layer and were likely organic rather than skeletal bound Ba and were therefore excluded from further discussion (Figure S4 in Supporting Information S1). Strong seasonality is observed for Ba/Ca in both cores, with minimum Ba/Ca occurring between November to January and a maximum from May to September (Figures 4 and 5). The seasonal Ba/Ca cycle ranges from  $\sim 4$  to  $\sim 15$   $\mu\text{mol/mol}$  in magnitude. Once seasonal cycles were removed, the remaining Ba/Ca record from the forereef FR-12 (i.e., up to February 2007) displays a significant increasing trend through time (Cox-Stuart,  $p \ll 0.01$ ,  $n = 1018$ ), evident in the loess curve in Figure 4. Initially below the backreef Ba/Ca at the start of the 1920s, the long-term forereef Ba/Ca quickly equals and overtakes backreef values by the 1950s. The backreef BR-06 Ba/Ca record is relatively stable for much of the studied interval, showing a small upward step (Cox-Stuart,  $p = 0.02$ ,  $n = 1188$ ) in the 1990s (Buishand range test, 1993,  $p = 0.0028$ ), considerably later than the Ba/Ca increases in the forereef. Using a periodogram on detrended Ba/Ca without seasonality, three apparent sets of cycles were identified in both cores (Figure S2 in Supporting Information S1): (a) between 2 and 7 years, (b) between 8 and 12 years and (c) a longer cycle between 18 and 25 years.

### 3.2. Coral Luminescence

The fluorescence profiles from both cores exhibit clear seasonal cycles akin to Ba/Ca with a minimum from November to January and a maximum from May to September (Figure 5). FR-12 provides values from May 1922 to February 2007 (Figure 6), whilst BR-06 yields values from May 1908 to April 2007.

### 3.3. Pearson's R Correlations and Cross-Correlations (CCF)

Inter-sample Ba/Ca and luminescence Pearson's correlation coefficients between the backreef and forereef corals are 0.26 ( $p < 0.01$ ,  $n = 504$ ) and 0.12 ( $p = 0.01$ ,  $n = 504$ ), respectively. The Ba/Ca between the two cores has a significant correlation, but the correlation is not strong. This suggests that while the cores have similar seasonal cyclicity (Figure S3 in Supporting Information S1), they are likely reflecting different magnitudes due to the different sources of Ba/Ca to the backreef and forereef. Intra-sample Ba/Ca and luminescence and in situ temperature correlation coefficients were also calculated. Correlation coefficients for Ba/Ca<sub>Backreef</sub> versus luminescence<sub>Backreef</sub> and in situ temperature were 0.25 ( $p < 0.01$ ,  $n = 594$ ) and 0.34 ( $p < 0.01$ ,  $n = 197$ ), respectively. Correlation coefficients for Ba/Ca<sub>Forereef</sub> versus luminescence<sub>Forereef</sub> and in situ temperature were 0.19 ( $p < 0.01$ ,  $n = 504$ ) and 0.54 ( $p < 0.01$ ,  $n = 197$ ), respectively.

Cross-correlation plots between the FR-12 and BR-06 colonies were constructed to highlight the covariation between Ba/Ca and luminescence (Figure S3 in Supporting Information S1). Highest correlation between Ba/Ca and luminescence occurs at  $t \sim 0$  years (i.e., no time lag between proxies), with positive correlations at yearly intervals and negative correlations at half-year intervals, suggesting directly proportional interannual (i.e., long-term) and seasonal trends between the two tracers.

## 4. Discussion

### 4.1. [Ba/Ca]<sub>seawater</sub>, Calcification, and Temperature Controls on Ba/Ca<sub>coral</sub>

Coral skeletal Ba/Ca is known to be influenced by organic non-carbonate bound barium (Marks et al., 2017; Sinclair et al., 1998; Tudhope et al., 1996). Sinclair et al. (1998) observed organic enrichments of Ba/Ca on the outer edges of the coral skeleton, agreeing with our data that displays extreme Ba/Ca peaks at the top of the coral core, coinciding with the discolored tissue layer (Marks et al., 2017) (see Figure S4 in Supporting Information S1). These extreme peaks ( $>1000 \mu\text{mol/mol}$ ) starkly contrast the rest of the data in the cores ( $\sim 4\text{--}20 \mu\text{mol/mol}$ ). Given the lack of discoloration below the tissue layer, we suggest the Ba/Ca variability is not caused by organic bound barium past the core top. This is confirmed by the agreement between Ba/Ca of oxidatively cleaned powder samples measured by solution ICP-MS and Ba/Ca of the uncleaned samples measured by laser ablation (Figure 3).

Corals precipitate their skeletons from an extracellular calcifying fluid (ECF) semi-isolated from seawater (Cohen & McConnaughey, 2003). A number of processes could modify the composition of the ECF during calcification, including Rayleigh fractionation of the ECF (Gaetani et al., 2011; Tambutte et al., 2011). Rayleigh fractionation occurs as progressive precipitation of aragonite leaves the residual ECF proportionally enriched or depleted in its elemental ratio in relation to calcium depending on the partition coefficient ( $K_D$ ) of the trace element in question ( $x$  in Equation 1). Elements like Ba with  $K_D > 1$  (e.g., Ba  $K_D$  between 2.11 and 1.30 at 25°C (Gaetani & Cohen, 2006; Lea et al., 1989)) are preferentially taken into the skeleton, thus reducing its concentrations with respect to Ca in the residual ECF and in subsequently precipitated aragonite. Conversely, a coral skeletal element with  $K_D \ll 1$ , for example, Mg, will progressively increase in the ECF and increase in the coral skeleton with mass of aragonite precipitated (Gagnon et al., 2007). In this way, coral Ba/Ca may not just depend on Ba/Ca<sub>sw</sub>, but also on the internal calcification mechanisms related to  $K_D$ , such as temperature, calcification rate, and seawater exchange rate (Venn et al., 2020).

$$K_D^x = \frac{D_{\text{Aragonite-Seawater}}^x}{D_{\text{Ca}}^{\text{Aragonite-Seawater}}} \quad (1)$$

$$\ln \frac{\text{Ba}}{\text{Ca}} = \frac{2337 \pm 270}{T} - 5.3 \pm 0.9 \quad (2)$$

If Rayleigh fractionation were a dominant process controlling the variations in Ba/Ca data, a well-defined negative correlation between Ba/Ca and Mg/Ca within each coral would be expected. Yearly Ba/Ca and Mg/Ca averages are plotted alongside theoretical coral Rayleigh fractionation curves defined using the approach of Stewart et al. (2016) with two different estimates for the  $K_D$  of Ba and varying [Ba] in the initial calcifying fluid (Figure S7 in Supporting Information S1). The lack of correlation between the Ba/Ca and Mg/Ca indicates that the relative variations in Ba/Ca data are not driven by Rayleigh fractionation factors and periodically replenishing

ECF. Furthermore, in both cases, the concentration of Ba in the ECF must be more than 50% higher than average Atlantic surface seawater (Chan et al. (1977)) or Honduran coastal waters (Carilli, Prouty, et al. (2009)) for a Rayleigh curve to fall close to our data (Figure S7 in Supporting Information S1). Thus, it seems likely that an external factor other than Rayleigh fractionation of the ECF is driving the observed variation in skeletal Ba/Ca through time.

The dependence of  $K_D$  on ambient temperature of the calcifying fluid could impart additional environmental sensitivity to the Ba/Ca. Calibrations suggest an inverse dependence of  $Ba^{2+}$  incorporation in aragonite with temperature (Dietzel et al., 2004; Gaetani & Cohen, 2006; Lea et al., 1989). Although seasonal cycles in SST exist in the Sapodilla Cayes, they are relatively minor at these sites (26°C to 30°C winter to summer (Fowell et al., 2016)), thus minimizing potential temperature influence on Ba/Ca. Using the calibration (Equation 2) from Gaetani and Cohen (2006), the summer to winter temperature difference would result in a variation of Ba/Ca of less than 1.4  $\mu\text{mol/mol}$ , therefore it cannot explain our observed seasonality and would furthermore imply lowest Ba/Ca during warmer months, which is opposite to that observed. Similarly, a 1°C increase in mean summertime SST over the entire core timespan (Fowell et al., 2016), would act to decrease Ba/Ca by  $\sim 0.3 \mu\text{mol/mol}$ , thus the  $>6 \mu\text{mol/mol}$  increase over the timespan of the forereef coral may in fact slightly underestimate changes due to fluvial input.

Counter to the negative relationship between temperature and Rayleigh-fractionation-driven coral aragonite Ba/Ca modeled by Gaetani and Cohen (2006), SST in the present study exhibits a strong positive correlation with Ba/Ca over the time period for which in situ data are available (forereef  $r^2 = 0.54$ ,  $p \ll 0.01$ ; backreef  $r^2 = 0.34$ ,  $p \ll 0.01$ ; Figure S5 in Supporting Information S1). This is true for the majority of the core based on the monthly means in Figure 5, which show peak Ba/Ca occurring during the summer months when SST also peaks (LaVigne et al., 2016; Tanzil et al., 2019). This correlation, however, is unlikely a causative relationship. The wet season and warm season are broadly synchronous on the MBRS (Figure 5), likely providing the common factor between temperature and Ba/Ca. Moreover, owing to how the age model was constructed, where the Ba/Ca was tuned to the first peak of the wet season (July–August), there is a possibility that correlation between the temperature and coral Ba/Ca is an artifact that requires an independent age model to resolve. Furthermore, if temperature was an important controlling factor, the two cores would be expected to exhibit more similar long-term Ba/Ca evolution than they do given their comparable warming histories (Fowell et al., 2016).

Based on these considerations, we conclude that the observed Ba/Ca trends reflect changes in  $Ba/Ca_{sw}$ , and the temporal trends exhibited are largely unrelated to a change in the  $K_D$  of Ba between coral skeletal aragonite and seawater. This is consistent with the recent study by Chalk et al. (2021) that suggested that Ba/Ca in *S. siderea* had a dominant environmental driver. The cycles are large for Ba/Ca in corals but corroborates earlier studies of *S. siderea* that exhibit larger variations in Ba/Ca compared to other species of coral (Reuer et al., 2003).

#### 4.2. Changes in $Ba/Ca_{sw}$

In recent years, seasonality in  $[Ba]_{sw}$  has been attributed to a variety of natural processes such as ocean productivity and wet/dry season river/groundwater discharge rates. Ocean productivity often negatively correlates with Ba/Ca in shallow water corals as Ba is scavenged out of the water column during periods of higher total productivity (Carter et al., 2020). Within the local waters of the coral collection sites, remote sensing records of chlorophyll-a concentrations suggest that productivity peaks during the wet season in the MBRS (June–November). Thus, the productivity peak overlaps with the Ba/Ca coral peak (Figure 5)—the opposite of what is expected if productivity alone was driving the availability of Ba in the water column. This suggests that another process dominated our observed  $Ba/Ca_{sw}$  seasonality.

Both rivers and groundwater are sources of Ba to reef waters. Specifically, within this study region river plumes of sediment have been observed to reach the southern MBRS from Sea-viewing Wide Field-of-view Sensor SeaWiFS Ocean colour images (Andrefouet et al., 2002), even with the corals at 30–40 km from the coast. There is no direct evidence or local proxy to test the effect of groundwater content on the  $[Ba]_{sw}$  in this region—a potential line of inquiry for a future study. There are, however, some limited river discharge data from the Rio Humuya, which ultimately flows into the Ulúa, which correlates strongly with precipitation rate ( $R = 0.76$ ,  $n = 156$ ,  $p \ll 0.01$ ) and hence the observed trends in coral Ba/Ca. Direct covariation between Ba/Ca and river discharge is also evident in Figure 6, albeit with some chronological mismatch which could be attributed to constructing the age-model with a sixth-order polynomial that does not completely account for short-term variations in skeletal



extension rate. However, discharge and precipitation both peak during the wet season alongside our Ba/Ca from both cores (June–November, Figure 5). Thus, river discharge with increased sediment loads, and [Ba], during the wet season are entirely compatible with the Ba/Ca patterns we observe within the two coral cores.

In addition to delivering Ba to reefs, rivers are a primary source of humic-like acids that cause fluorescence within coral skeletons (Boto & Isdale, 1985; Grove et al., 2012). Coral luminescence is therefore a robust proxy for riverine flux (Grove et al., 2013; Lough, 2011a; Sinclair & McCulloch, 2004). After long-term trends in the luminescence are removed, which are an artefact of progressive backfilling of the coral skeleton (Lough, 2011b), we find a significant weak to moderate correlation between luminescence and Ba/Ca (Figure S9 in Supporting Information S1 and Figure 6), with Pearson's R correlations of 0.19 ( $p \ll 0.01$ ,  $n = 504$ ) and 0.25 ( $p \ll 0.01$ ,  $n = 594$ ) for the forereef and backreef corals, respectively. However, Pearson's R tests the correlation between both covariation and magnitude. Given that luminescence and Ba/Ca variations are caused by the uptake of different materials, which are believed to both be driven by riverine supply albeit by different carriers, it is not necessarily correct to assume that luminescence and Ba/Ca magnitudes will respond similarly every time there is a change in riverine supply. Instead, cross-correlation, where the correlation between the two profiles is measured at successive time lags between them, was used to determine that the strongest correlation between luminescence and Ba/Ca occurs with 0 lag years for both the backreef and the forereef, suggesting that humic acid and Ba were concordantly delivered to the coral (Figure S3 in Supporting Information S1). This is also evident in the monthly means where both luminescence and Ba/Ca peak within the summer months (Figure 5). The statistical significance of this covariation supports the temporal connection between riverine flux and the delivery of humic-like acids (causing fluorescence) and Ba to the reef, but the relatively low magnitude of the correlation suggests that Ba/Ca and luminescence do not always respond in a linear fashion to changes in riverine flux. Accordingly, within this study, only changes in Ba/Ca are interpreted as a proxy of sediment delivery to the reef waters of the coral.

### 4.3. Ba/Ca and the MBRS Hydroclimate

Three major trends were identified in the Ba/Ca transects; (a) seasonal variations we associate with the wet and dry seasonality (Figure 5); (b) interannual variations unrelated to seasonality that are ascribed to climate cycles (Figure S2 in Supporting Information S1); and (c) the increase in Ba/Ca over the last 80-year, which is much more pronounced in the forereef than in the backreef colony (Figure 4). We interpret only the first two trends to be associated with the MBRS hydroclimate variations.

Albeit sometimes site-specific, the positive relationship between coral Ba/Ca and local precipitation connected by the link of river discharge and riverine sediment delivery, is well established (Brenner et al., 2017; Horta-Puga & Carriquiry, 2012; Maina et al., 2012). The hydroclimate and precipitation patterns of the MBRS are dominated by the annual shift of the ITCZ. This process is recorded in the observed Ba/Ca data as seasonal oscillations with peak values that coincide with the wet season (Figure 5). Furthermore, the MBRS hydroclimate experiences lower frequency cycles in climate modulating weather parameters, such as wind shear (ENSO; Mestas-Nunez and Enfield, 2007), atmospheric pressure (CLLJ; Caribbean Low-Level Jet; Whyte et al., 2008), and SSTs (Atlantic Multidecadal Oscillation, Pacific Decadal Oscillation; Taylor et al., 2002) that enhance and weaken evaporation and precipitation. The high spatial resolution of LA-ICP-MS ( $\mu\text{m}$ ) in this study allows a more detailed analysis of the short-term variability of coral element profiles and the recent hydroclimate.

Periodogram analysis of Ba/Ca in both the forereef and backreef resulted in 3 apparently distinct cycles (Figure S2 in Supporting Information S1). We relate these to the effects of climate cycles on regional precipitation and can thus be seen in Ba/Ca given the correlation between precipitation and discharge rates in the MBRS as discussed in Section 4.2. The first is a 2-to-7 years cycle, which at this lower frequency, may relate to ENSO which increases rainfall in Central America from increased wind shear driving warmer equatorial waters eastwards enhancing evaporation and precipitation, and thus affecting Ba/Ca delivery from rivers. Additionally this lower frequency cycle could relate to the strong CLLJ with increased sea level pressures and suppressed rainfall that decreases Ba/Ca periodically (Enfield et al., 2001; Mestas-Nunez & Enfield, 2007; Whyte et al., 2008). The second is an 8–12 years cycle, separate from ENSO, related to slower oscillations in the North Atlantic and tropical Atlantic SSTs also enhancing precipitation periodically (Jury, 2009). A third multi-decadal cycle ( $\sim 18$ –25 years) could potentially be associated with the AMO and its relationship with the Atlantic warm pool and evaporation (Klotzbach, 2011). The presence of these cycles within our records, which are known to impact regional precipitation patterns (Jury, 2009; Mestas-Nunez & Enfield, 2007; Taylor et al., 2002), supports the existence of a



relationship between the regional hydroclimate and the Ba/Ca of the studied coral skeletons. The semblance of the regional climate cycles represented in both the forereef and backreef Ba/Ca indicate that both colonies are under the same hydroclimate regime, and the different rivers themselves do not cause disparities in the Ba/Ca, but rather cause variations in Ba/Ca via the supply of Ba to the corals. Relating Ba/Ca to long-term variability in hydroclimate reinforces the use of this proxy for long-term riverine flux to the reef.

#### 4.4. Long-Term Increases in Ba/Ca and Coral Decline

The initial study from Castillo et al. (2011) shows that the rates of extension of forereef *S. siderea* colonies on the MBRS in Belize ( $n = 7$ ) have been steadily declining since the 1930's, while corals from the backreef show a much more stable growth trend ( $n = 3$ ). The cause of variability in growth trends in corals of the same species in such close geographic proximity is unclear. Changing extension rates can be a good proxy for coral health and, given the concurrence between multiple corals, this suggests that corals from the forereef of the MBRS in Belize have experienced more decline than those of the backreef. Figure 4 shows the extension for FR-12 and BR-06 alongside Ba/Ca profiles. FR-12 has significant negative trend (Cox-Stuart,  $p = 0.002$ ,  $n = 94$ ) and BR-06 has a significant positive trend (Cox-Stuart,  $p = 0.0002$ ,  $n = 82$ ). We note that the imperfect slabbing of our individual coral cores (i.e., not perfectly parallel to the polyp growth axis) can lead to over-estimation of absolute extension (DeLong et al., 2016), and a changing angle of slabbing can cause apparent changes in extension rate over the core. However, the consistent pattern of extension trends between seven forereef and three backreef corals suggests that coral cutting technique did not impact the overall findings of the Castillo et al. (2011) study. It is highly unlikely that all forereef cores were exclusively cut at an angle decreasing extension from the top to bottom, while all backreef cores were cut at an angle increasing extension. To achieve an overall change in extension of  $\sim 6$  mm/year to  $\sim 4$  mm/year, observed in the forereef FR-12 core within this study, would require a change in slab angle from the top to the bottom of the core of  $48^\circ$  between the coral slab and axis of growth (Yudelman & Slowey, 2022). Such a large change is not evident in the luminescence or X-rays images (Figures S1 and S10 in Supporting Information S1). Another notable limitation to the use of extension rates as indicators for coral health is that even within a species, individual colonies can respond differently to the same stressors. Again, however, the concurrent analyses from different colonies from the same reef suggests that, in this case, the corals on the MBRS are responding in the same manner to some common environmental driver. Furthermore, the decline in forereef corals is also observed for other mounding coral species in the Sapodilla Cayes, such as *Montastraea faveolata* (Carilli, Norris, et al., 2009). Thus, long-term extension decline in the forereef over the last 80 years corresponds well with the increasing Ba/Ca trend in this coral (Figure 4).

In contrast to regional precipitation, which is thought to have increased uniformly across the Caribbean during the last century (Stephenson et al., 2014), our two Ba/Ca records exhibit diverging long-term trends. The backreef Ba/Ca trend shows a slight increase later in the core (1990s), while the forereef Ba/Ca provides a more discernible increase of  $>70\%$  across the last 100 years, with a breakpoint in the 1950s (Figure 4). Collectively, the association between Ba/Ca in these corals and riverine discharge to the reef, the close proximity of the corals, and their common hydroclimate, suggest that the increase in only the forereef reflects differing Ba input to the forereef and backreef environments. River-borne sediments are dispersed and diluted in the open ocean, hence,  $Ba/Ca_{sw}$  ought to show a gradient decreasing with distance from the coastline (Carilli, Prouty, et al., 2009; Castillo et al., 2011; Prouty et al., 2008). If the Sapodilla Cayes reefs followed this pattern, backreef Ba/Ca should be generally higher than forereef Ba/Ca due to their relative proximity to land (Figure 1). This gradient is observed in the data at the start of 20<sup>th</sup> century, but as the backreef Ba/Ca remains stable thereafter, the forereef Ba/Ca converges on backreef Ba/Ca in the 1930s, and ultimately surpasses backreef Ba/Ca by the 1950s (Figure 4). This result appears to stem from an increase in sediment delivery to the forereef versus the backreef owing to a more pronounced secular increase in riverine sediment input to the forereef environment through time.

Sediment delivery to the southern MBRS is dominated by river input from the much larger watersheds of Honduras (Ulúa,  $370 \text{ m}^3\text{s}^{-1}$  modeled discharge rate) and Guatemala, in addition to the Belizean rivers Monkey, Rio Grande, and Deep ( $49 \text{ m}^3\text{s}^{-1}$ ,  $35 \text{ m}^3\text{s}^{-1}$ , and  $16 \text{ m}^3\text{s}^{-1}$  respectively) (Burke & Sugg, 2006; Carilli, Prouty, et al., 2009; Castillo et al., 2011; Soto et al., 2009; Thattai et al., 2003). Overall, the river flux is highly weighted toward Honduras and it has been estimated that 80% of total sediment and 55% of total nutrients to the southern MBRS originate from Honduras, 16% of sediment and 25% of nutrients originate from Guatemala, and only 12% of nutrients and negligible sediment originate from Belize (Burke & Sugg, 2006; Cherubin et al., 2008). Ocean circulation in MBRS is generally to the northwest (counter-clockwise) from Honduras toward Mexico, but the

eastern Gulf of Honduras itself is a sediment retention area due to mesoscale eddies that entrap river flux and circle it back toward the coasts (Figure 1) (Cherubin et al., 2008; Ezer et al., 2005; Paris & Cherubin, 2008). Furthermore, for 7 months of the year, there is a southerly ocean current between the Belizean coast and the barrier reef shielding the backreef from strong fluxes of river input from Honduras. Rapid increases in human population in the last century, particularly in Honduras, have led to increases in deforestation and the use of fertilisers, herbicides, and pesticides (Figure 2) (United-Nations, 2020). Since the 1900's, it is estimated that the total runoff and river discharge from these countries has nearly doubled, resulting in a 20-fold increase in sediment delivery to coastal waters and considerable eutrophication (Burke & Sugg, 2006). It is likely that these increases are due to the anthropogenic changes in land use within the surrounding watersheds. The increased human pressures from Honduras have been highlighted by Carilli, Prouty, et al. (2009), who measured land-sourced trace-metal/Ca ratios (Mn/Ca, Cu/Ca, Sb/Ca, Ba/Ca, and Zn/Ca) in coral reefs living at varying distances from Honduras. This work revealed a positive relationship between trace-metal/Ca ratios and proximity to Honduras, suggesting that mainland Honduras is the dominant source of these trace metals in the MBRS. This, along with patterns of circulation, suggest that the forereef is currently subject to the much larger and more sediment-rich riverine load from Honduras, while the backreef receives smaller riverine loads from Belize. This supports the hypothesis that the decline in skeletal extension of the forereef coral, which was not exhibited by the backreef coral, is related to an increasing supply of sediment and possibly other contaminants to the forereef environment from Honduran rivers.

The increase in sediment load to the forereef over the last century inferred from the Ba/Ca proxy data would likely have been associated with a concomitant increase in nutrient load to the reef. Net ecosystem production in the forereef has been linked with the ca. 8-year quasi-decadal cycle (Fowell et al., 2018) that is evident in the Ba/Ca data. A general trend of increasing net ecosystem production and decreasing net ecosystem calcification on the forereef relative to the backreef over the last 100 years has also been documented using paired  $\delta^{11}\text{B}$  and  $\delta^{13}\text{C}$  of *S. siderea* skeleton (Fowell et al., 2018). Although a direct link is perhaps difficult to establish at this stage, it is possible this may be a consequence of enhanced riverine sediment and nutrient supply to the forereef, driving Ba/Ca higher, and stimulating ecosystem-level productivity of non-calcifiers (e.g., fleshy macroalgae). These correlations therefore offer a potential explanation for the declining health of the forereef corals of the MBRS (as measured by linear extension) and, if replicated in other studies, may account for wider trends in coral decline across the Caribbean.

## 5. Conclusions

Here we present more than 80 years of Ba/Ca data from two *S. siderea* corals from proximal forereef and backreef environments of the southern MBRS. The forereef coral exhibits a gradual increase in overall Ba/Ca, while the backreef coral exhibits similarly stable Ba/Ca through time. With little evidence for temperature or Rayleigh-type effects on skeletal Ba/Ca, we conclude that Ba/Ca from both samples within this study were overwhelmingly influenced by changing  $\text{Ba/Ca}_{\text{sw}}$ .

Luminescence profiles from each coral track observed Ba/Ca cycles, with both cycles tied strongly to riverine discharge to the reef. Ba/Ca is therefore similarly equated to changes in riverine flux and sediment load delivery to the reef, with peak Ba/Ca occurring during the wet season. Both Ba/Ca profiles exhibit similar lower frequency climate cycles, potentially linked to ENSO and the quasi-decadal cycle common in the region, suggesting that a difference in hydroclimate (i.e., rainfall increase) alone is not likely responsible for the increase in Ba/Ca that was observed in the forereef coral, but not in the backreef coral. Instead, given that the coral with a declining extension rate from the forereef receives considerably more riverine input from Honduras, a difference in sediment load can explain the different long-term Ba/Ca trends observed. We propose that a gradual increase in sediment supply to this part of the reef associated with coastal land-use changes in Honduras played a role in the decline in health of the forereef corals on the MBRS, as evidenced by decreasing linear extension rates (Castillo et al., 2011), and had less impact on backreef corals of the MBRS, for which sediment load is primarily derived from less populated Belize. Our results highlight the importance of watershed management for safeguarding reef health and the contrasting ways in which different parts of a single reef system can be impacted by local and regional stressors.

## Data Availability Statement

Supporting analytical Data Sets (S1–S6) are available at <https://doi.org/10.1594/PANGAEA.938752> (Shaw et al., 2023). River discharge data are available via an online form request from The Global Runoff Data Centre, 56068 Koblenz, Germany ([https://www.bafg.de/GRDC/EN/Home/homepage\\_node.html](https://www.bafg.de/GRDC/EN/Home/homepage_node.html)). Rainfall data are freely available from the CEDA Archive (University-of-East-Anglia-Climatic-Research-Unit et al., 2021).

## Acknowledgments

Andy Milton is acknowledged for his mass spectrometry support. This research was partly funded by a Leverhulme Trust grant and a Royal Society Wolfson Merit award to G.L.F. and by an Advanced ERC grant Microns2Reefs (884650) to GLF. The collection and preparation of the coral cores were funded by NOAA award NA13OAR4310186 (to J.B.R. and K.D.C.) and NSF award 1437371 (to J.B.R.). Permits for collection and export were granted by the Belize Fisheries Department, Government of Belize.

## References

- Andrefouet, S., Mumby, P. J., McField, M., Hu, C., & Muller-Karger, F. E. (2002). Revisiting coral reef connectivity. *Coral Reefs*, 21(1), 43–48. <https://doi.org/10.1007/s00338-001-0199-0>
- Baker, D. M., Webster, K. L., & Kim, K. (2010). Caribbean octocorals record changing carbon and nitrogen sources from 1862 to 2005. *Global Change Biology*, 16(10), 2701–2710. <https://doi.org/10.1111/j.1365-2486.2010.02167.x>
- Boto, K., & Isdale, P. (1985). Fluorescent bands in massive corals result from terrestrial fulvic-acid inputs to nearshore zone. *Nature*, 315(6018), 396–397. <https://doi.org/10.1038/315396a0>
- Boyle, E. A. (1981). Cadmium, zinc, copper, and barium in foraminifera tests. *Earth and Planetary Science Letters*, 53(1), 11–35. [https://doi.org/10.1016/0012-821x\(81\)90022-4](https://doi.org/10.1016/0012-821x(81)90022-4)
- Brenner, L. D., Linsley, B. K., & Dunbar, R. B. (2017). Examining the utility of coral Ba/Ca as a proxy for river discharge and hydroclimate variability at Coiba Island, Gulf of Chiriqui, Panama. *Marine Pollution Bulletin*, 118(1–2), 48–56. <https://doi.org/10.1016/j.marpolbul.2017.02.013>
- Burke, L., & Sugg, Z. (2006). In W. R. Insitute (Ed.), *Hydrologic modelling of watersheds discharging adjacent to the Mesoamerican Reef*.  
Cardoso, G. O., Falsarella, L. N., Chiroque-Solano, P. M., Porcher, C. C., Leitzke, F. P., Wegner, A. C., et al. (2022). Coral growth bands recorded trace elements associated with the Fundao dam collapse. *Science of the Total Environment*, 807, 150880. <https://doi.org/10.1016/j.scitotenv.2021.150880>
- Carilli, J. E., Norris, R. D., Black, B. A., Walsh, S. M., & McField, M. (2009). Local stressors reduce coral resilience to bleaching. *PLoS One*, 4(7), e6324. <https://doi.org/10.1371/journal.pone.0006324>
- Carilli, J. E., Prouty, N. G., Hughen, K. A., & Norris, R. D. (2009). Century-scale records of land-based activities recorded in Mesoamerican coral cores. *Marine Pollution Bulletin*, 58(12), 1835–1842. <https://doi.org/10.1016/j.marpolbul.2009.07.024>
- Carricart-Ganivet, J. P., Vasquez-Bedoya, L. F., Cabanillas-Teran, N., & Blanchon, P. (2013). Gender-related differences in the apparent timing of skeletal density bands in the reef-building coral *Siderastrea siderea*. *Coral Reefs*, 32(3), 769–777. <https://doi.org/10.1007/s00338-013-1028-y>
- Carriquiry, J. D., & Horta-Puga, G. (2010). The Ba/Ca record of corals from the Southern Gulf of Mexico: Contributions from land-use changes, fluvial discharge and oil-drilling muds. *Marine Pollution Bulletin*, 60(9), 1625–1630. <https://doi.org/10.1016/j.marpolbul.2010.06.007>
- Carter, S. C., Paytan, A., & Griffith, E. M. (2020). Toward an improved understanding of the marine barium cycle and the application of marine barite as a paleoproductivity proxy. *Minerals*, 10(5), 421. <https://doi.org/10.3390/min10050421>
- Castillo, K. D., & Lima, F. P. (2010). Comparison of in situ and satellite-derived (MODIS-Aqua/Terra) methods for assessing temperatures on coral reefs. *Limnology and Oceanography: Methods*, 8(3), 107–117. <https://doi.org/10.4319/lom.2010.8.0107>
- Castillo, K. D., Ries, J. B., & Weiss, J. M. (2011). Declining coral skeletal extension for forereef colonies of *Siderastrea siderea* on the mesoamerican barrier reef system, southern Belize. *PLoS One*, 6(2), e14615. <https://doi.org/10.1371/journal.pone.0014615>
- Castillo, K. D., Ries, J. B., Weiss, J. M., & Lima, F. P. (2012). Decline of forereef corals in response to recent warming linked to history of thermal exposure. *Nature Climate Change*, 2(10), 756–760. <https://doi.org/10.1038/nclimate1577>
- Chalk, T. B., Standish, C. D., D'Angelo, C., Castillo, K. D., Milton, J. A., & Foster, G. L. (2021). Mapping coral calcification strategies from in situ boron isotope and trace element measurements of the tropical coral *Siderastrea siderea*. *Scientific Reports*, 11(1), 472. <https://doi.org/10.1038/s41598-020-78778-1>
- Chan, D. D., Edmond, J. M., & Grant, B. (1977). Barium data from Atlantic GEOSECS expedition. *Deep-Sea Research*, 24(7), 613–649. [https://doi.org/10.1016/0146-6291\(77\)90505-7](https://doi.org/10.1016/0146-6291(77)90505-7)
- Cherubin, L. M., Kuchinke, C. P., & Paris, C. B. (2008). Ocean circulation and terrestrial runoff dynamics in the Mesoamerican region from spectral optimization of SeaWiFS data and a high resolution simulation. *Coral Reefs*, 27(3), 503–519. <https://doi.org/10.1007/s00338-007-0348-1>
- Cohen, A. L., & McConnaughey, T. A. (2003). Geochemical perspectives on coral mineralization. In P. M. Dove, J. J. DeYoreo, & S. Weiner (Eds.), *Reviews in mineralogy and geochemistry, Biomineralization* (Vol. 54, pp. 151–187). <https://doi.org/10.2113/0540151>
- Cramer, K. L., Jackson, J. B. C., Donovan, M. K., Greenstein, B. J., Korpanty, C. A., Cook, G. M., & Pandolfi, J. M. (2020). Widespread loss of Caribbean acroporid corals was underway before coral bleaching and disease outbreaks. *Science Advances*, 6(17). <https://doi.org/10.1126/sciadv.aax9395>
- De'ath, G., Lough, J. M., & Fabricius, K. E. (2009). Declining coral calcification on the Great Barrier Reef. *Science*, 323(5910), 116–119. <https://doi.org/10.1126/science.1165283>
- DeLong, K. L., Flannery, J. A., Maupin, C. R., Poore, R. Z., & Quinn, T. M. (2011). A coral Sr/Ca calibration and replication study of two massive corals from the Gulf of Mexico. *Paleoceanography, Paleoclimatology, Palaeoecology*, 307(1–4), 117–128. <https://doi.org/10.1016/j.palaeo.2011.05.005>
- DeLong, K. L., Maupin, C. R., Flannery, J. A., Quinn, T. M., & Shen, C. C. (2016). Refining temperature reconstructions with the Atlantic coral *Siderastrea siderea*. *Paleoceanography, Paleoclimatology, Palaeoecology*, 462, 1–15. <https://doi.org/10.1016/j.palaeo.2016.08.028>
- Dietzel, M., Gussone, N., & Eisenhauer, A. (2004). Co-precipitation of Sr<sup>2+</sup> and Ba<sup>2+</sup> with aragonite by membrane diffusion of CO<sub>2</sub> between 10 and 50 degrees C. *Chemical Geology*, 203(1–2), 139–151. <https://doi.org/10.1016/j.chemgeo.2003.09.008>
- Enfield, D. B., Mestas-Nunez, A. M., & Trimble, P. J. (2001). The Atlantic multidecadal oscillation and its relation to rainfall and river flows in the continental US. *Geophysical Research Letters*, 28(10), 2077–2080. <https://doi.org/10.1029/2000gl012745>
- Evans, D., & Muller, W. (2018). Automated extraction of a five-year LA-ICP-MS trace element data set of ten common glass and carbonate reference materials: Long-term data quality, optimisation and laser cell homogeneity. *Geostandards and Geoanalytical Research*, 42(2), 159–188. <https://doi.org/10.1111/ggr.12204>
- Ezer, T., Thattai, D. V., Kjerfve, B., & Heyman, W. D. (2005). On the variability of the flow along the Meso-American Barrier Reef system: A numerical model study of the influence of the Caribbean current and eddies. *Ocean Dynamics*, 55(5–6), 458–475. <https://doi.org/10.1007/s10236-005-0033-2>

- Fabrizius, K. E. (2005). Effects of terrestrial runoff on the ecology of corals and coral reefs: Review and synthesis. *Marine Pollution Bulletin*, 50(2), 125–146. <https://doi.org/10.1016/j.marpolbul.2004.11.028>
- Fowell, S. E., Foster, G. L., Ries, J. B., Castillo, K. D., de la Vega, E., Tyrrell, T., et al. (2018). Historical trends in pH and carbonate biogeochemistry on the Belize Mesoamerican Barrier Reef system. *Geophysical Research Letters*, 45(7), 3228–3237. <https://doi.org/10.1002/2017gl076496>
- Fowell, S. E., Sandford, K., Stewart, J. A., Castillo, K. D., Ries, J. B., & Foster, G. L. (2016). Intrareef variations in Li/Mg and Sr/Ca sea surface temperature proxies in the Caribbean reef-building coral *Siderastrea siderea*. *Paleoceanography*, 31(10), 1315–1329. <https://doi.org/10.1002/2016pa002968>
- Gaetani, G. A., & Cohen, A. L. (2006). Element partitioning during precipitation of aragonite from seawater: A framework for understanding paleoproxies. *Geochimica et Cosmochimica Acta*, 70(18), 4617–4634. <https://doi.org/10.1016/j.gca.2006.07.008>
- Gaetani, G. A., Cohen, A. L., Wang, Z. R., & Crusius, J. (2011). Rayleigh-based, multi-element coral thermometry: A biomineralization approach to developing climate proxies. *Geochimica et Cosmochimica Acta*, 75(7), 1920–1932. <https://doi.org/10.1016/j.gca.2011.01.010>
- Gagnon, A. C., Adkins, J. F., Fernandez, D. P., & Robinson, L. F. (2007). Sr/Ca and Mg/Ca vital effects correlated with skeletal architecture in a scleractinian deep-sea coral and the role of Rayleigh fractionation. *Earth and Planetary Science Letters*, 261(1–2), 280–295. <https://doi.org/10.1016/j.epsl.2007.07.013>
- GRDC. (2022). The Global Runoff Data Centre. Retrieved from [https://www.bafg.de/GRDC/EN/Home/homepage\\_node.html](https://www.bafg.de/GRDC/EN/Home/homepage_node.html)
- Grove, C. A., Nagtegaal, R., Zinke, J., Scheufen, T., Koster, B., Kasper, S., et al. (2010). River runoff reconstructions from novel spectral luminescence scanning of massive coral skeletons. *Coral Reefs*, 29(3), 579–591. <https://doi.org/10.1007/s00338-010-0629-y>
- Grove, C. A., Zinke, J., Peeters, F., Park, W., Scheufen, T., Kasper, S., et al. (2013). Madagascar corals reveal a multidecadal signature of rainfall and river runoff since 1708. *Climate of the Past*, 9(2), 641–656. <https://doi.org/10.5194/cp-9-641-2013>
- Grove, C. A., Zinke, J., Scheufen, T., Maina, J., Epping, E., Boer, W., et al. (2012). Spatial linkages between coral proxies of terrestrial runoff across a large embayment in Madagascar. *Biogeosciences*, 9(8), 3063–3081. <https://doi.org/10.5194/bg-9-3063-2012>
- Guzman, H. M., & Jimenez, C. E. (1992). Contamination of coral reefs by heavy-metals along the the Caribbean coast of Central-America (Costa-Rica and Panama). *Marine Pollution Bulletin*, 24(11), 554–561. [https://doi.org/10.1016/0025-326x\(92\)90708-e](https://doi.org/10.1016/0025-326x(92)90708-e)
- Guzman, H. M., & Tudhope, A. W. (1998). Seasonal variation in skeletal extension rate and stable isotopic (C-13/C-12 and O-18/O-16) composition in response to several environmental variables in the Caribbean reef coral *Siderastrea siderea*. *Marine Ecology Progress Series*, 166, 109–118. <https://doi.org/10.3354/meps166109>
- Hammer, Ø., Harper, D. A. T., & Ryan, P. D. (2001). PAST: Paleontological statistics software package for education and data analysis [Software]. In *Palaeontologia electronica* (Vol. 1). Retrieved from [https://palaeo-electronica.org/2001\\_1/past/issue1\\_01.htm](https://palaeo-electronica.org/2001_1/past/issue1_01.htm)
- Hanor, J. S., & Chan, L. H. (1977). Non-conservative behavior of barium during mixing of Mississippi river and Gulf of Mexico waters. *Earth and Planetary Science Letters*, 37(2), 242–250. [https://doi.org/10.1016/0012-821x\(77\)90169-8](https://doi.org/10.1016/0012-821x(77)90169-8)
- Harris, I., Osborn, T. J., Jones, P., & Lister, D. (2020). Version 4 of the CRU TS monthly high-resolution gridded multivariate climate dataset. *Scientific Data*, 7(1), 109. <https://doi.org/10.1038/s41597-020-0453-3>
- Hathorne, E. C., Gagnon, A., Felis, T., Adkins, J., Asami, R., Boer, W., et al. (2013). Interlaboratory study for coral Sr/Ca and other element/Ca ratio measurements. *Geochemistry, Geophysics, Geosystems*, 14(9), 3730–3750. <https://doi.org/10.1002/ggge.20230>
- Hoegh-Guldberg, O., Mumby, P. J., Hooten, A. J., Steneck, R. S., Greenfield, P., Gomez, E., et al. (2007). Coral reefs under rapid climate change and ocean acidification. *Science*, 318(5857), 1737–1742. <https://doi.org/10.1126/science.1152509>
- Horel, J. D. (1982). On the annual cycle of the tropical pacific atmosphere and ocean. *Monthly Weather Review*, 110(12), 1863–1878. [https://doi.org/10.1175/1520-0493\(1982\)110<1863:otacot>2.0.co;2](https://doi.org/10.1175/1520-0493(1982)110<1863:otacot>2.0.co;2)
- Horta-Puga, G., & Carriquiry, J. D. (2012). Coral Ba/Ca molar ratios as a proxy of precipitation in the northern Yucatan Peninsula, Mexico. *Applied Geochemistry*, 27(8), 1579–1586. <https://doi.org/10.1016/j.apgeochem.2012.05.008>
- Jackson, J. B. C., Donovan, J. K., Cramer, K. L., & Lam, V. Y. Y. (2014). Status and trends of Caribbean coral reefs: 1970–2012. In *Global coral reef monitoring network*. IUCN.
- Jury, M. R. (2009). A quasi-decadal cycle in Caribbean climate. *Journal of Geophysical Research*, 114(D13). <https://doi.org/10.1029/2009jd011741>
- Kaushal, N., Yang, L. D. Q., Tanzil, J. T. I., Lee, J. N., Goodkin, N. F., & Martin, P. (2020). Sub-annual fluorescence measurements of coral skeleton: Relationship between skeletal luminescence and terrestrial humic-like substances. *Coral Reefs*, 39(5), 1257–1272. <https://doi.org/10.1007/s00338-020-01959-x>
- Klotzbach, P. J. (2011). The influence of El Niño-Southern Oscillation and the Atlantic Multidecadal oscillation on Caribbean tropical cyclone activity. *Journal of Climate*, 24(3), 721–731. <https://doi.org/10.1175/2010jcli3705.1>
- Knowlton, N., & Jackson, J. B. C. (2008). Shifting baselines, local impacts, and global change on coral reefs. *PLoS Biology*, 6(2), 215–220. <https://doi.org/10.1371/journal.pbio.0060054>
- LaVigne, M., Grotoli, A. G., Palardy, J. E., & Sherrell, R. M. (2016). Multi-colony calibrations of coral Ba/Ca with a contemporaneous in situ seawater barium record. *Geochimica et Cosmochimica Acta*, 179, 203–216. <https://doi.org/10.1016/j.gca.2015.12.038>
- LaVigne, M., Hill, T. M., Spero, H. J., & Guilderson, T. P. (2011). Bamboo coral Ba/Ca: Calibration of a new deep ocean refractory nutrient proxy. *Earth and Planetary Science Letters*, 312(3–4), 506–515. <https://doi.org/10.1016/j.epsl.2011.10.013>
- Lea, D. W., Shen, G. T., & Boyle, E. A. (1989). Coralline barium records temporal variability in Equatorial Pacific upwelling. *Nature*, 340(6232), 373–376. <https://doi.org/10.1038/340373a0>
- Lewis, S. E., Lough, J. M., Cantin, N. E., Matson, E. G., Kinsley, L., Bainbridge, Z. T., & Brodie, J. E. (2018). A critical evaluation of coral Ba/Ca, Mn/Ca and Y/Ca ratios as indicators of terrestrial input: New data from the Great Barrier Reef, Australia. *Geochimica et Cosmochimica Acta*, 237, 131–154. <https://doi.org/10.1016/j.gca.2018.06.017>
- Lough, J. M. (2011a). Great Barrier Reef coral luminescence reveals rainfall variability over northeastern Australia since the 17th century. *Paleoceanography*, 26(2). <https://doi.org/10.1029/2010pa002050>
- Lough, J. M. (2011b). Measured coral luminescence as a freshwater proxy: Comparison with visual indices and a potential age artefact. *Coral Reefs*, 30(1), 169–182. <https://doi.org/10.1007/s00338-010-0688-0>
- Maina, J., de Moel, H., Vermaat, J. E., Bruggemann, J. H., Guillaume, M. M. M., Grove, C. A., et al. (2012). Linking coral river runoff proxies with climate variability, hydrology and land-use in Madagascar catchments. *Marine Pollution Bulletin*, 64(10), 2047–2059. <https://doi.org/10.1016/j.marpolbul.2012.06.027>
- Marchitto, T. M. (2006). Precise multielemental ratios in small foraminiferal samples determined by sector field ICP-MS. *Geochemistry, Geophysics, Geosystems*, 7(5). <https://doi.org/10.1029/2005gc001018>
- Marks, G. S., LaVigne, M., Hill, T. M., Sauthoff, W., Guilderson, T. P., Roark, E. B., et al. (2017). Reproducibility of Ba/Ca variations recorded by northeast Pacific bamboo corals. *Paleoceanography*, 32(9), 966–979. <https://doi.org/10.1002/2017pa003178>



- McCulloch, M., Fallon, S., Wyndham, T., Hendy, E., Lough, J., & Barnes, D. (2003). Coral record of increased sediment flux to the inner Great Barrier Reef since European settlement. *Nature*, *421*(6924), 727–730. <https://doi.org/10.1038/nature01361>
- Mestas-Nunez, A. M., Enfield, D. B., & Zhang, C. (2007). Water vapor fluxes over the Intra-Americas Sea: Seasonal and interannual variability and associations with rainfall. *Journal of Climate*, *20*(9), 1910–1922. <https://doi.org/10.1175/jcli4096.1>
- Ogden, J. C., & Ogden, N. B. (1998). Reconnaissance survey of the coral reefs and associated ecosystems of Cayos Cochinos, Honduras. *Revista de Biología Tropical*, *46*, 67–74.
- Okai, T., Suzuki, A., Kawahata, H., Terashima, S., & Imai, N. (2002). Preparation of a new Geological Survey of Japan geochemical reference material: Coral JcP-1. *Geostandards Newsletter-the Journal of Geostandards and Geoanalysis*, *26*(1), 95–99. <https://doi.org/10.1111/j.1751-908x.2002.tb00627.x>
- Ourbak, T., Corregge, T., Malaize, B., Le Cornec, F., Charlier, K., & Peypouquet, J. P. (2006). A high-resolution investigation of temperature, salinity, and upwelling activity proxies in corals. *Geochemistry, Geophysics, Geosystems*, *7*(3). <https://doi.org/10.1029/2005gc001064>
- Paris, C. B., & Cherubin, L. M. (2008). River-Reef connectivity in the Meso-American region. *Coral Reefs*, *27*(4), 773–781. <https://doi.org/10.1007/s00338-008-0396-1>
- Pretet, C., Reynaud, S., Ferrier-Pages, C., Gattuso, J. P., Kamber, B. S., & Samankassou, E. (2014). Effect of salinity on the skeletal chemistry of cultured scleractinian zooxanthellate corals: Cd/Ca ratio as a potential proxy for salinity reconstruction. *Coral Reefs*, *33*(1), 169–180. <https://doi.org/10.1007/s00338-013-1098-x>
- Prouty, N. G., Field, M. E., Stock, J. D., Jupiter, S. D., & McCulloch, M. (2010). Coral Ba/Ca records of sediment input to the fringing reef of the southshore of Molokai, Hawaii' over the last several decades. *Marine Pollution Bulletin*, *60*(10), 1822–1835. <https://doi.org/10.1016/j.marpolbul.2010.05.024>
- Prouty, N. G., Huguen, K. A., & Carilli, J. (2008). Geochemical signature of land-based activities in Caribbean coral surface samples. *Coral Reefs*, *27*(4), 727–742. <https://doi.org/10.1007/s00338-008-0413-4>
- R-Core-Team. (2019). *A language and environment for statistical computing*. R Foundation for Statistical Computing.
- Reuer, M. K., Boyle, E. A., & Cole, J. E. (2003). A mid-twentieth century reduction in tropical upwelling inferred from coralline trace element proxies. *Earth and Planetary Science Letters*, *210*(3–4), 437–452. [https://doi.org/10.1016/s0012-821x\(03\)00162-6](https://doi.org/10.1016/s0012-821x(03)00162-6)
- Rogers, C. S. (1983). Sublethal and lethal effects of sediments applied to common Caribbean reef corals in the field. *Marine Pollution Bulletin*, *14*(10), 378–382. [https://doi.org/10.1016/0025-326x\(83\)90602-1](https://doi.org/10.1016/0025-326x(83)90602-1)
- Rogers, C. S. (1990). Responses of coral reefs and reef organisms to sedimentation. *Marine Ecology Progress Series*, *62*(1–2), 185–202. <https://doi.org/10.3354/meps062185>
- Rosenheim, B. E., Swart, P. K., & Thorrold, S. R. (2005). Minor and trace elements in sclerosponge *Ceratoporella nicholsoni*: Biogenic aragonite near the inorganic endmember? *Palaeogeography, Palaeoclimatology, Palaeoecology*, *228*(1–2), 109–129. <https://doi.org/10.1016/j.palaeo.2005.03.055>
- Saha, N., Webb, G. E., Zhao, J. X., Leonard, N. D., & Nguyen, A. D. (2018). Influence of marine biochemical cycles on seasonal variation of Ba/Ca in the near-shore coral *Cyphastrea*, Rat Island, southern Great Barrier Reef. *Chemical Geology*, *499*, 71–83. <https://doi.org/10.1016/j.chemgeo.2018.09.005>
- Sathyendranath, S., Brewin, R. J. W., Brockmann, C., Brotas, V., Calton, B., Chuprin, A., et al. (2019). An ocean-colour time series for use in climate studies: The experience of the Ocean-Colour Climate Change Initiative (OC-CCI). *Sensors*, *19*(19), 4285. Retrieved from <https://www.mdpi.com/1424-8220/19/19/4285>
- Shaw, K. M. M., Foster, G. L., Standish, C. D., Fowell, S. E., Stewart, J. A., Castillo, K. D., & Ries, J. B. (2021). Ba/Ca coral data from century-long records of sedimentary input on a Caribbean reef from coral Ba/Ca ratios: Linking coral health and land use [Dataset]. *PANGAEA*. <https://doi.org/10.1594/PANGAEA.938752>
- Sinclair, D. J. (2005). Non-river flood barium signals in the skeletons of corals from coastal Queensland, Australia. *Earth and Planetary Science Letters*, *237*(3–4), 354–369. <https://doi.org/10.1016/j.epsl.2005.06.039>
- Sinclair, D. J., Kinsley, L. P. J., & McCulloch, M. T. (1998). High resolution analysis of trace elements in corals by laser ablation ICP-MS. *Geochimica et Cosmochimica Acta*, *62*(11), 1889–1901. [https://doi.org/10.1016/s0016-7037\(98\)00112-4](https://doi.org/10.1016/s0016-7037(98)00112-4)
- Sinclair, D. J., & McCulloch, M. T. (2004). Corals record low mobile barium concentrations in the Burdekin river during the 1974 flood: Evidence for limited Ba supply to rivers? *Palaeogeography, Palaeoclimatology, Palaeoecology*, *214*(1–2), 155–174. <https://doi.org/10.1016/j.palaeo.2004.07.028>
- Sinclair, D. J., Williams, B., Allard, G., Ghaleb, B., Fallon, S., Ross, S. W., & Risk, M. (2011). Reproducibility of trace element profiles in a specimen of the deep-water bamboo coral *Keratoisis* sp. *Geochimica et Cosmochimica Acta*, *75*(18), 5101–5121. <https://doi.org/10.1016/j.gca.2011.05.012>
- Soto, I., Andrefouet, S., Hu, C., Muller-Karger, F. E., Wall, C. C., Sheng, J., & Hatcher, B. G. (2009). Physical connectivity in the Mesoamerican Barrier Reef System inferred from 9 years of ocean color observations. *Coral Reefs*, *28*(2), 415–425. <https://doi.org/10.1007/s00338-009-0465-0>
- Spooner, P. T., Robinson, L. F., Hemsing, F., Morris, P., & Stewart, J. A. (2018). Extended calibration of cold-water coral Ba/Ca using multiple genera and co-located measurements of dissolved barium concentration. *Chemical Geology*, *499*, 100–110. <https://doi.org/10.1016/j.chemgeo.2018.09.012>
- Stephenson, T. S., Vincent, L. A., Allen, T., Van Meerbeek, C. J., McLean, N., Peterson, T. C., et al. (2014). Changes in extreme temperature and precipitation in the Caribbean region, 1961–2010. *International Journal of Climatology*, *34*(9), 2957–2971. <https://doi.org/10.1002/joc.3889>
- Stewart, J. A., Anagnostou, E., & Foster, G. L. (2016). An improved boron isotope pH proxy calibration for the deep-sea coral *Desmophyllum dianthus* through sub-sampling of fibrous aragonite. *Chemical Geology*, *447*, 148–160.
- Sutherland, K. P., Porter, J. W., Turner, J. W., Thomas, B. J., Looney, E. E., Luna, T. P., et al. (2010). Human sewage identified as likely source of white pox disease of the threatened Caribbean Elkhorn coral, *Acropora palmata*. *Environmental Microbiology*, *12*(5), 1122–1131. <https://doi.org/10.1111/j.1462-2920.2010.02152.x>
- Sylvester, P. (2008). Matrix effects in laser ablation ICP-MS In. *Laser ablation ICP-MS in the Earth sciences: Current practices and outstanding issues* (Vol. 40, pp. 67–78). Mineralogical Association of Canada.
- Tambutte, S., Holcomb, M., Ferrier-Pages, C., Reynaud, S., Tambutte, E., Zoccola, D., & Allemand, D. (2011). Coral biomineralization: From the gene to the environment. *Journal of Experimental Marine Biology and Ecology*, *408*(1–2), 58–78. <https://doi.org/10.1016/j.jembe.2011.07.026>
- Tanzil, J. T. I., Goodkin, N. F., Sin, T. M., Chen, M. L., Fabbro, G. N., Boyle, E. A., et al. (2019). Multi-colony coral skeletal Ba/Ca from Singapore's turbid urban reefs: Relationship with contemporaneous in situ seawater parameters. *Geochimica et Cosmochimica Acta*, *250*, 191–208. <https://doi.org/10.1016/j.gca.2019.01.034>
- Taylor, M. A., Enfield, D. B., & Chen, A. A. (2002). Influence of the tropical Atlantic versus the tropical Pacific on Caribbean rainfall. *Journal of Geophysical Research*, *107*(C9), 10-1–10-14. <https://doi.org/10.1029/2001jc001097>



- Thattai, D., Kjerfve, R., & Heyman, W. D. (2003). Hydrometeorology and variability of water discharge and sediment load in the inner Gulf of Honduras, western Caribbean. *Journal of Hydrometeorology*, 4(6), 985–995. [https://doi.org/10.1175/1525-7541\(2003\)004<0985:havowd>2.0.co;2](https://doi.org/10.1175/1525-7541(2003)004<0985:havowd>2.0.co;2)
- Pohlert, T. (2020). trend: Non-parametric trend tests and change-point detection [Software]. Retrieved from <https://cran.r-project.org/web/packages/trend/trend.pdf>
- Trapletti, A., & Hornik, K. (2020). tseries: Time series analysis and computational finance [Software]. Retrieved from <https://cran.r-project.org/web/packages/tseries/tseries.pdf>
- Tudhope, A. W., Lea, D. W., Shimmield, G. B., Chilcott, C. P., & Head, S. (1996). Monsoon climate and Arabian Sea coastal upwelling recorded in massive corals from southern Oman. *PALAIOS*, 11(4), 347–361. <https://doi.org/10.2307/3515245>
- United-Nations. (2020). FAOSTAT 2020. In *Food and agriculture of the united nations*.
- University-of-East-Anglia-Climatic-Research-Unit, Harris, I., Jones, P., & Osborn, T. (2021). CRU TS4. 05: Climatic Research Unit (CRU) Time-Series (TS) version 4.05 of high-resolution gridded data of month-by-month variation in climate (Jan. 1901–Dec. 2020) [Dataset]. *NERC EDS Centre for Environmental Data Analysis*. Retrieved from <https://catalogue.ceda.ac.uk/uuid/c26a65020a5e4b80b20018f148556681>
- Venn, A. A., Bernardet, C., Chabenat, A., Tambutte, E., & Tambutte, S. (2020). Paracellular transport to the coral calcifying medium: Effects of environmental parameters. *Journal of Experimental Biology*, 223(17). <https://doi.org/10.1242/jeb.227074>
- Weerabaddana, M. M., DeLong, K. L., Wagner, A. J., Loke, D. W. Y., Kilbourne, K. H., Slowey, N., et al. (2021). Insights from barium variability in a *Siderastrea siderea* coral in the northwestern Gulf of Mexico. *Marine Pollution Bulletin*, 173, 112930. <https://doi.org/10.1016/j.marpolbul.2021.112930>
- Whyte, F. S., Taylor, M. A., Stephenson, T. S., & Campbell, J. D. (2008). Features of the Caribbean low level jet. *International Journal of Climatology*, 28(1), 119–128. <https://doi.org/10.1002/joc.1510>
- Yudelman, E. A., & Slowey, N. C. (2022). Coral extension rate analysis using computed axial tomography. *Coral Reefs*, 41(4), 973–985. <https://doi.org/10.1007/s00338-022-02235-w>